Plant Science 358 (2025) 112567

Contents lists available at ScienceDirect

Plant Science

journal homepage: www.elsevier.com/locate/plantsci

Endoplasmic reticulum activation via tunicamycin seed priming enhances salt acclimation in rice seedlings

Francisco Dalton Barreto de Oliveira [a,b], Isabelle Mary Costa Pereira [a,b,c], Igor Rafael Sousa Costa [a,b], Francisco Lucas Pacheco Cavalcante [a,b], Ítalo Antônio Cotta Coutinho [d], Murilo Siqueira Alves [a], Stelamaris de Oliveira Paula-Marinho [a,b], Eneas Gomes-Filho [a,b], Humberto Henrique de Carvalho [a,b,c,*]

[a] Departamento de Bioquímica e Biologia Molecular, Bloco 907, Universidade Federal do Ceará - Campus do Pici, Fortaleza, CE CEP: 60451-970, Brazil
[b] INCT AgriS, Instituto Nacional de Ciência e Tecnologia em Agricultura Sustentável no Semiárido Tropical. Departamento de Engenharia Agrícola, Bloco 804, Universidade Federal do Ceará - Campus do Pici, Fortaleza, CE CEP: 60440-554, Brazil
[c] ForCE Metabolomics, Fortaleza, CE, 60451-970, Brazil
[d] Departamento de Biologia, Bloco 906, Universidade Federal do Ceará - Campus do Pici, Fortaleza, CE CEP: 60356-900, Brazil

ARTICLE INFO

Keywords:
Seed priming
Tunicamycin
Antioxidants
Oryza sativa L.
Metabolic profiles

ABSTRACT

Seed priming is a promising approach to increasing salt acclimation, but the role of endoplasmic reticulum (ER) remains unclear. This study investigated if ER activation by tunicamycin (TM) as a seed priming agent promotes salt acclimation in rice (*Oryza sativa* L.) seedlings. The results showed that salinity (150 mM NaCl) decreased the seedling growth. However, priming seeds with TM increased dry mass, length, photosynthetic pigments and K^+ contents, osmotic potential, and antioxidant enzyme activities under salinity. Conversely, it decreased intracellular Na^+ accumulation, electrolyte leakage, lipid peroxidation, and ROS levels. Additionally, TM priming enhanced the expression of ER response gene markers *OsIRE1*, *OsbZIP50,* and *OsbZIP60* in seedlings under salinity. Metabolomic profiling revealed that TM priming and salinity positively modulated salt-defensive metabolites in shoots, including the osmoprotectants β-alanine and maltose. In roots, it led to a higher accumulation of phosphoric acid, the amino acids O-acetylserine and N-acetylserine (involved in Fe and S metabolism), and the sugars maltose, raffinose, and sorbitol, which also function as osmoprotectants and energy sources. In conclusion, TM seed priming followed by salt stress activated ER unfolded protein response (UPR). This may enhance antioxidant enzyme activity, reducing ROS levels and intracellular Na^+ content, thereby mitigating salt stress through the positive modulation of defense-related and energy-related metabolites. These findings suggest an efficient strategy to improve salt acclimation during the early growth stages of rice seedlings.

1. Introduction

Adverse conditions such as pathogen attacks, heat, salinity, drought, or exposure to specific chemicals, including the natural antibiotic tunicamycin (TM), can lead to the accumulation of unfolded or misfolded proteins in the endoplasmic reticulum (ER) lumen, a state known as ER stress (Je et al., 2023; Park and Park, 2019a; Liu et al., 2025). It triggers a cytoprotective, nucleus-integrated pathway known as the unfolded protein response (UPR). The UPR involves transcription factors, proteases, and RNase activities to re-establish ER homeostasis, maintaining the quality control of exported proteins (Manghwar and Li, 2022).

In plants, UPR involves two main branches (Ayaz et al., 2024). The first one includes a Basic Leucine Zipper 60 (bZIP60) protein and an RNA splicing factor protein, the inositol-requiring enzyme 1 (IRE1), which has an N-terminal sensor domain facing the ER lumen and a C-terminal end facing the cytosol (Liu et al., 2022a; Mishiba et al., 2019). The other one comprises membrane-associated transcription factors, such as the

* Corresponding author at: Departamento de Bioquímica e Biologia Molecular, Bloco 907, Universidade Federal do Ceará - Campus do Pici, Fortaleza, CE CEP: 60451-970, Brazil.
E-mail addresses: italo.coutinho@ufc.br (Í.A.C. Coutinho), murilo.alves@ufc.br (M.S. Alves), humberto.carvalho@ufc.br (H.H. Carvalho).

https://doi.org/10.1016/j.plantsci.2025.112567
Received 3 April 2025; Received in revised form 13 May 2025; Accepted 16 May 2025
Available online 18 May 2025

bZIP17 and bZIP28 proteins (Bao et al., 2019). Under stress conditions, IRE1 detects misfolded proteins in the ER lumen, leading to its dimerization and activation of RNase function. It catalyzes the alternative cytoplasmic splicing of the bZIP60 transcription factor (Mishiba et al., 2019). In the nucleus, the bZIP60 protein upregulates the expression of genes encoding various native ER chaperones, such as binding protein (BiP), which helps to decrease ER stress (Nagashima et al., 2011). Additionally, bZIP17 and bZIP28 migrate to the Golgi complex, where their transmembrane domains are cleaved, enabling their transcription factor domains to enter the nucleus and activate the chaperone's expression. Like bZIP60, these transcription factors enhance protein processing or, in severe cases, activate programmed cell death (Ayaz et al., 2024; Nawkar et al., 2018). Such membrane components have been described in *Arabidopsis thaliana* and conserved among crops such as rice, soybean, and maize. In rice, only one ortholog of each has been recognized (Howell, 2021; Hayashi et al., 2013): *Os*IRE1 is the *At*IRE1a/b isoform (Hayashi et al., 2012), *At*bZIP60 is *Os*bZIP50, also known as *Os*bZIP74 (Lu et al., 2012), the isoform of *At*bZIP17 is *Os*bZIP17 also known as *Os*bZIP39, and for *At*bZIP28 is *Os*bZIP60 also known as *Os*bZIP16 (Hayashi et al., 2012; Yang et al., 2022).

Several studies have examined the impact of ER stress on plant metabolism. TM aggravates stress effects with prolonged exposure, leading to decreased expression of IRE1 and BiP chaperones, suppression of metabolic pathways related to primary metabolism, and impaired seedling growth (Lima et al., 2022). However, moderate ER stress is associated with plant biomass maintenance, positive modulation of primary metabolites (such as glycolysis and TCA cycle intermediates), and increased ER-related gene expression (e.g., *BiP* and *IRE1*). In contrast, excessive stress induces effects such as reduced growth (Cavalcante et al., 2023). Additionally, low to moderate levels of ER stress may handle the UPR pathway to mitigate the harmful effects of environmental stress on cells, enhancing the tolerance response and increasing plant performance under saline stress (Beaugelin et al., 2020; Ohta and Takaiwa, 2020). One evidence of this is that ER stress induced by chemicals reduces sodium accumulation in *Sorghum bicolor*, and it may be related to the increase in the expression of *SOS* genes in roots (de Queiroz et al., 2020). Beyond ER stress, salinity can also lead to an overproduction of reactive oxygen species (ROS), which causes oxidative stress and disrupts the chloroplast electron transport chain (Singh, 2022). This oxidative imbalance results in protein oxidation, DNA damage, and, most notably, lipid peroxidation in membranes (Hasanuzzaman et al., 2020). To counteract these effects, cells have developed an antioxidant system comprised of non-enzymatic compounds, such as phenolic compounds, ascorbic acid, and carotenoids (Laxa et al., 2019), and antioxidant enzymes (Kumari et al., 2022). Considering that most of these molecules (proteins) are synthesized in the ER, it is worth pointing out that this organelle is crucial for modulating plant stress responses (Kim et al., 2022). Since molecular responses to ER stress are not well comprehended in plants as in animals, studies that clarify these mechanisms are necessary (Howell, 2017).

Salinity is one of the most challenging environmental factors that affect crop yield, especially in arid and semiarid regions (Mukhopadhyay et al., 2021). It is widely known that salt stress can impair crucial cellular processes, such as photosynthesis (Ben Amor et al., 2020), cell wall integrity (Colin et al., 2023), and mitochondrial electron transport chain (Tang and Zhu, 2023), ultimately inhibiting plant growth and development (Zhao et al., 2021). In response to salt stress, plants have evolved physiological and biochemical mechanisms, such as the activation of mechanisms to control ionic homeostasis which include the reduction of Na^+ content in the cytosol, via compartmentation in the vacuole, carried out by antiport proteins called NHX, Na^+/H^+ exchanger (Bassil et al., 2019), or the efflux of this ion to the apoplast, performed by the SOS (Salt Overly Sensitive) antiporters (Ali et al., 2023). Besides its harmful effects on the cell, salinity induces several other secondary stresses, such as oxidative stress (Khan et al., 2022a) and ER stress by unfolded or misfolded protein accumulation (Çakır Aydemir et al., 2020). Under salt stress, ER sensors such as *AtbZIP17* act as transcription factors to control salt-responsive and UPR genes (Cho, 2024). Indeed, a crosstalk between salt tolerance and ER stress can be found in the capacity of ER to induce UPR pathways to recover from both stresses, a process related to ROS signaling (Li et al., 2021; Ozgur et al., 2018).

Several approaches have been applied to produce more tolerant crops to environmental stresses, such as priming agents, a short-period pretreating of seeds or leaves with biological, chemical, or physical agents to withstand severe stresses subsequently found (Méndez et al., 2016). Seed priming can induce physiological alterations, such as increased chlorophyll content, osmoprotectant levels, ROS, and defense metabolites that might lead to tolerance to abiotic stresses such as salinity (Brenya et al., 2023). Therefore, priming may contribute to more tolerant plant species through the generation of stress memory in important crops, such as rice (*Oryza sativa* L.) (Ganie et al., 2024). In this way, priming upregulates UPR and ER quality control genes, and their expression is maintained after recovery, enabling salt-primed plants to exhibit improved growth upon subsequent salt exposure (Tian et al., 2019).

Thus, we wondered if TM, an ER stress inducer, could act as a priming to induce salt acclimation in rice. Given this question, this work aimed to test the hypothesis that TM seed priming activates ER responses that help seedling establishment under salt stress. Understanding the responses of rice plants to abiotic stresses is crucial for breeding and genetic engineering programs, ultimately contributing to increased crop quality and yield, ensuring global food security, and promoting environmental sustainability.

2. Material and methods

2.1. Plant material and stress screenings

Rice seeds (*Oryza sativa* L.) of SCSBRS Tio Taka cultivar were provided by *Agrogiusti Indústria e Com. de Sementes Ltda.* (Turvo, SC, Brazil - 28° 56' 22.06222'' S, 49° 44' 9.64866" W). The experiment was carried out in a BOD (Biochemical Oxygen Demand) incubator with a mean temperature of 25 °C in a photoperiod of 12/12 h.

First, screening experiments were carried out to determine the optimal NaCl and Tunicamycin (TM) concentrations for further assays. The first and second ones were NaCl screenings, performed at the same time, with either 0 or 0.5 μg. mL^{-1} TM, being the latter chosen based on previous studies (Cavalcante et al., 2023). For this part, seeds were previously surface sanitized with a 0.5 % (v/v) sodium hypochlorite solution, washed three times with tap water, and rinsed with distilled water. Then, they were pre-treated at a fixed 0.5 μg. mL^{-1} TM for 24 hours (T050), or only with distilled water for 24 h (T0 as control group). They were dried at room temperature for 24 hours and sown in a moistened germitest paper. The first screening test used control (T0) rice seeds grown in crescent concentrations of NaCl (0, 100, 150, 200, and 250 mM NaCl), whereas the second one used 0.50 TM-primed seeds grown in the same five NaCl concentrations (0–250 mM). In this way, the seed germination was followed for 10 days (Lima et al., 2022). Based on the results, the NaCl concentration was fixed at 150 mM. Then, a third screening was performed using five distinct TM concentrations (0, 0.125, 0.250, 0.375, and 0.500 μg.mL^{-1}) submitted to 150 mM NaCl. Just like the two previous screening tests, seed germination tests were conducted in 10 days.

The following parameters were used to assess seed germination screenings: germination percentage, nº of abnormal seedlings, germination speed index (GSI) and shoot emergence speed index (SESI) (Maguire, 1962), mean shoot emergence time (MSET) and Mean germination time (MGT) (Labouriau, 1983). Additionally, after 10 days of sowing, we measured shoot length (SL), root length (RL), shoot dry mass (SDM), and root dry mass (RDM).

GSI = $\sum_{i=1}^{n} (\frac{Gi}{Ni})$, where:

Gi = number of germinated seeds counted per day
Ni = number of days after sowing
n = nth time (day) of counting
Mean germination time (MGT):
MGT = $\sum_{i=1}^{n}$Gi ∗ Ni/ΣGn, where:
Gi = number of seeds germinated per day of counting;
Ni = time between the first day of germination and the nth counting;
n = "nth" time (day) of counting

2.2. Seed pre-treatment and salt stress treatment establishment

According to the screening results, the next steps were performed using 0.25 μg.mL^{-1} TM as a seed pre-treatment and 150 mM NaCl as salt stress treatment during seed germination. Rice seeds were pre-treated with 0.25 μg.mL^{-1} TM (TM 0.25) for 24 h, after that left to dry at room temperature, and included a control group without priming. Then, seeds were sown in germination paper moistened to either 0 (distilled water) or 150 mM NaCl solution in a 2 × 2 factorial scheme. It was rolled and placed in the BOD incubator for 10 days in the same condition previously described. The germination papers were rewatered every 3 days to keep moist. Seedlings were evaluated after 10 days of sowing.

2.3. Seedling growth parameters

After this time, rice seedlings were collected and divided into shoots and roots for dry mass and length measurements. For length determination it was used the ImageJ software (Rasband et al., 2016), for dry masses, shoots and roots were placed in paper bags and transferred to a hot air oven, at 65 °C, for 3 days, until the uniform weight. After that, it was used an electronic scale for dry mass measurement.

2.4. Measurement of osmotic potential

The osmotic potential (Ψ_s) was measured in the xylem sap according (Callister et al., 2006). Approximately 350 mg of fresh shoot material was harvested and compressed with a disposable syringe. Then, the obtained extract was centrifuged at 6,000 × g for 5 min, and the supernatant used to determine the Ψ_s using the osmometer (VAPRO 5520, Wescor, Utah, USA), which provides molality values of the extracted saps, and the values were calculated using the Van't Hoff equation, and the values were expressed in MPa (Mega Pascal).

π = (- R). (T). (C.i), where:
π = osmotic pressure (MPa);
R = the universal gas constant (0.0821 L * atm* mole^{-1} * K^{-1});
C = the molal concentration of the solution (mmol. kg^{-1});
i = the Van't Hoff Fator (usually for ions is 1).

2.5. Electrolyte leakage

Electrolyte leakage (EL) was determined in rice shoots and roots (Dionisio-Sese and Tobita, 1998). Samples were incubated in deionized water, and the electrical conductivity 1 (EC1) was measured after 4 h using an electrical conductivity meter (Mp513, Sanxin®). The samples were then incubated in a water bath at 95 °C for 30 min to completely disrupt the plasma membrane, after which electrical conductivity was measured again (EC2). The percentage of EL was determined using the formula:

EL (%) = 100 × (EC1 / EC2).

2.6. Measurement of photosynthetic pigments

For the determination of photosynthetic pigment contents, approximately 25 mg of fresh tissues were incubated in 10 mL of dimethyl sulfoxide (DMSO) saturated with calcium carbonate ($CaCO_3$) to obtain the plant extract (Wellburn, 1994). After 24 h in the dark, samples were incubated at 65 °C for 45 min. The absorbance readings were obtained at 665, 649, and 480 nm in an Ultrospec 6300 pro spectrophotometer (Amersham Biosciences, Slough, United Kingdom). The pigment contents were expressed as mg. g^{-1} of dry mass using the following equations:

Chlorophyll a = [12.47 x (A_{665})] – [3.62 x (A_{649})]

Chlorophyll b = [25.06 x (A_{649})] – [6.50 x (A_{665})]

Total chlorophyll (a + b) = [7.15 x (A_{665})] – [18.71 x (A_{649})]

Carotenoids = {[1000 x (A_{480})] – [1.29 x (chlorophyll a)] – [53.78 (chlorophyll b)]} / 220

2.7. Inorganic ion contents

Inorganic ions were extracted by homogenizing 20 mg of dried and powdered rice shoots and roots in 2.0 mL of deionized water for 1.0 h at 75 °C, vortexing each sample every fifteen minutes. The homogenate was centrifuged at 3,000 × g for 10 min at room temperature. The Na^+ and K^+ and contents were determined by flame photometry (Malavolta et al., 1989). The ion Cl^- content was determined using a spectrophotometric method with NaCl as a standard and reaction with mercury (II) thiocyanate and iron (III) nitrate, with readings at 460 nm (Iwasaki et al., 1952). The contents were expressed as mg. g^{-1} of dry mass.

2.8. Detection of Na^+ by confocal microscopy

For the confocal microscopy analyses, root and shoot sections were placed on 0.01 M phosphate-buffered saline (PBS) at pH 7.4 (Sigma-Aldrich) and later incubated with a cell membrane-permeable cytosolic Na^+ indicator, 5 μM Asante NaTRIUM Green-2 AM, for 1.0 h in the dark based on literature (Gadelha et al., 2021; Roder and Hille, 2014). Fluorescence emission by Asante NaTRIUM Green-2 AM was collected from 535 to 555 nm, resulting in interaction between the probe and the ion sodium. The root was standardized as the root hair zone for all samples (Lima et al., 2022), and the leaf was the median region furthest from the edges, since seedlings have only one root and one pair of leaves.

Sections were washed three times for 5 min with PBS and incubated with Calcofluor White (0.2 μg/mL) (Fluorescent Brightener 28, Sigma, UK) for 5 min in the dark. Fluorescence emission by calcofluor white is blue and indicates cellulose in the cell walls. They were washed three times each 5 min with PBS at pH 7.4, and sealed with coverslip sealant (CoverGrip™ Biotium - Fisher Scientific). Samples were analyzed on a confocal scanning laser microscope (LSM710, Carl Zeiss, Jena) using appropriate lasers. Images were captured with Zen software (Zeiss). For measuring the mean intensity of emission of NaTRIUM Green-2AM, three image captures for each treatment, an unstained (not treated with any dye) image was kept in potassium phosphate-buffered saline only to capture natural fluorescence. The 3 layers of fluorescence intensity was measured using Zen software. The intensities were quantified using the entire image, deducting blank (buffer + sample) to minimize shadow effects caused by the interaction of the buffer with the probe.

2.9. Lipid peroxidation

Lipid peroxidation was measured by evaluating the

malondialdehyde (MDA) absorbance (Heath and Packer, 1968). Fresh rice shoots and roots (0.2 g) were macerated in 5 % trichloroacetic acid (TCA) at 4 °C. After centrifugation at 10,000 × g for 15 min, an aliquot of the supernatant was mixed with a solution of 0.5 % (w/v) thiobarbituric acid (TBA) in 20 % (w/v) TCA and then heated at 95 °C in a water bath for 30 min. MDA content was calculated based on the difference in absorbance at 532 and 600 nm, using a molar extinction coefficient of 155 $mM^{-1} \cdot cm^{-1}$, expressed in μmol MDA $\cdot g^{-1}$ of fresh mass.

2.10. Reactive oxygen species contents ($\cdot O_2^-$ and H_2O_2)

Crude extracts were prepared by homogenizing 0.2 g of fresh mass from shoots and roots in 50 mM potassium phosphate buffer (pH 7.8) and 0.1 % (w/v) TCA, with 5 mM KCN, respectively, for superoxide radical ($\bullet O_2^-$) and hydrogen peroxide (H_2O_2) extraction (Cheeseman, 2006; Xu et al., 2010). Spectrophotometric readings at 530 nm were performed on the supernatant to measure superoxide ($\bullet O_2^-$) content using a $NaNO_2$ solution as the standard curve (Elstner and Heupel, 1976). For determining H_2O_2 concentration, a standard curve was prepared with H_2O_2 solutions, potassium phosphate (pH 7.0), and potassium iodide (Sergiev et al., 1997).

2.11. Antioxidant enzymes

For antioxidant enzyme activities, 0.2 g of rice shoots and roots were homogenized in 100 mM phosphate buffer (pH 7.0) with 0.1 mM ethylenediaminetetraacetic acid (EDTA) at 4 °C. After centrifugation at 12,000 × g at 4 °C, the supernatant was collected and used to measure the enzyme activity. Protein concentration in the raw extracts was determined using bovine serum albumin (BSA) as standard (Bradford, 1976).

Enzyme activities were assayed in a 96-well microplate reader (Synergy HTX, BioTek®), performing a kinetic activity over 30 min at 30 °C, except for superoxide dismutase (SOD; EC 1.15.1.1), which was performed in a glass cuvette using a spectrophotometer. Absorbance decay of ascorbate peroxidase (APX; EC 1.11.1.11) was measured at 290 nm, and the activity was calculated using the molar extinction coefficient for ascorbate ($\varepsilon = 2.8\ mM^{-1}.cm^{-1}$) (Nakano and Asada, 1981). Catalase (CAT; EC 1.11.1.6) activity was determined by consumption of H_2O_2 monitored at 240 nm using the molar extinction coefficient ($\varepsilon = 36\ M^{-1}.\ cm^{-1}$) (Beers and Sizer, 1952). Guaiacol peroxidase (GPOD; EC 1.11.1.7) activity was measured using the molar extinction coefficient for tetraguaiacol ($\varepsilon = 26.6\ mM^{-1}.\ cm^{-1}$) (Urbanek et al., 1991). APX, CAT, and GPOD activities were expressed as μmol H_2O_2. min^{-1}. g $protein^{-1}$. SOD activity was measured by absorbance reading of blue formazan at 560 nm, produced by photoreduction of the nitroblue tetrazolium (NBT), after 15 min under light (two 20-W fluorescent tubes) at 25 °C (Beyer and Fridovich, 1987). SOD activity was determined as the amount of enzyme required to cause 50 % inhibition of the NBT photoreduction, it was expressed as enzyme unit (U. g $protein^{-1}$).

2.12. Expression analysis by qPCR

Total RNA was isolated using TRizol (Sigma Aldrich), the quantification and integrity checked in a NanoDrop 2000 spectrophotometer (Thermo Scientific TM, Waltham, USA), and electrophoresis in a 1.5 % (m/v) agarose gel electrophoresis system, at 50 mA, 100 V. cDNA libraries were built employing M-MLV reverse transcriptase. Reverse transcription-polymerase chain reaction (RT-PCR) was performed using RNase-free water and oligo(dT)s incubation at 70 °C for 5 min and cooling at 4 °C for 5 min. It was mixed with RNase inhibitor, Reverse Transcription Mix, oligo(dTs) and submitted to 25 °C annealing temperature for 5 min, followed by elongation at 42 °C for 60 min and enzyme denaturation at 70 °C for 15 min. Synthesized cDNA was stored under −20 °C until used. The qPCR amplifications were carried out in a real-time thermal cycler (Esco Swift, Esco), composed of initial denaturation at 95 °C for 2 min and 40 thermal cycles of 15 s at 95 °C, followed by 15 s at a specific annealing temperature for each primer (Supplementary Table S1) and finally at 20 s at 60 °C in a total volume of 10 μL, according to the manufacturer's instructions of GoTaq qPCR Master Mix (Promega) in biological triplicates.

The efficiency of the primers was determined by the serial dilution method of cDNAs and calculated based on the slope, with values obtained between 95 % and 100 %. Melting curves confirmed the absence of nonspecific products and dimer formation. The relative quantification of transcripts was performed using the mean (Livak and Schmittgen, 2001).

2.13. Metabolic profiles by Gas chromatography coupled to mass spectrometry (GC-MS)

Approximately 50 mg of the samples were ground and mixed in methanol, chloroform, and ultrapure water (2: 1: 2, v/v) solution for polar metabolite extraction (Lisec et al., 2006). Then, 30 μL of the internal standard ribitol (0.2 mg mL^{-1}) was added to the mixture, and 150 μl aliquot of the upper (polar) water-methanol phase was transferred to a new tube and dried in a vacuum concentrator at room temperature (SpeedVac Concentrator, Eppendorf, Hamburg, Germany). In the derivatization stage, the dried samples were treated with methoxylamine hydrochloride (10 mg / 0.5 mL in pyridine) with stirring at 37 °C for 2 h, followed by the addition of N-methyl-N-(trimethylsilyl)-trifluoro acetamide (MSTFA) with stirring at 37 °C for 30 min. Then, the samples were conducted for GC-MS analyses.

GC–MS analyses were carried out on a QP–PLUS 2010 Shimadzu GC–MS instrument. One microliter of the sample was injected in split mode (1:10 ratio) with helium as carrier gas at a flow rate of 1.0 mL $.min^{-1}$ in an RTX-5MS capillary column (30 mm # 0.25 mm # 0.25 μm) to separate the metabolites. Chromatographic runs were carried out in five replicates at 80 °C for 5 min, then increased to 310 °C by 8 °C.$min^{-1}$and maintained for 1 min at this temperature. The injection, ions source, and MS interface temperatures were 230, 200, and 250 °C, respectively. The mass spectrometer was operated at 70 eV (EI) in a scanning range of 80–700 (m/z), initiated after a solvent cut-off time of 4.0 min. Chromatograms and mass spectra were processed using the Xcalibur™ 2.1 software (Thermo Fisher Scientific). Metabolites were identified based on the comparison of their retention times and fragmentation patterns of amino acids, carbohydrates, and organic acids previously obtained (Lima et al., 2022; Cavalcante et al., 2023; Costa et al., 2023), internal MS library composed of metabolite standards, and Golm's metabolome database Arabidopsis fragmentation patterns (http://gmd.mpimp-golm.mpg.de/analysisinput.aspx). The relative value of each metabolite was determined by dividing their respective peak areas by the internal standard ribitol peak area, then dividing by the fresh mass of the sample. Then, metabolites were identified and classified using the Kyoto Gene and Genome Encyclopedia (KEGG) or the PubChem databases.

2.14. Experimental design and statistical analysis

The experiment comprised a completely randomized design. For the NaCl screening, two sets of experiments were performed, both with five NaCl levels (0, 100, 150, 200, and 250 mM) treatments: the first one was performed without TM (unprimed seeds), and in the second one seeds were primed with 0.500 $\mu g.mL^{-1}$, to determine the most appropriate NaCl concentration for 2 × 2 experiments. The experiment was carried out from 5 TM-primed treatments (TM 0, 0.125, 0.250, 0.375, and 0.500), with 4 repetitions per treatment and 50 rice seeds for each repetition, with NaCl at 150 mM, to determine the best TM concentration for further analyses. Data were submitted to regression analysis using the Sisvar Software (Ferreira, 2011). The outcome of this analysis was obtained through linear, quadratic, and cubic polynomial regressions, at a 5 % probability level, adjusted for all variables.

After the screening tests, all further analyses were carried out with a

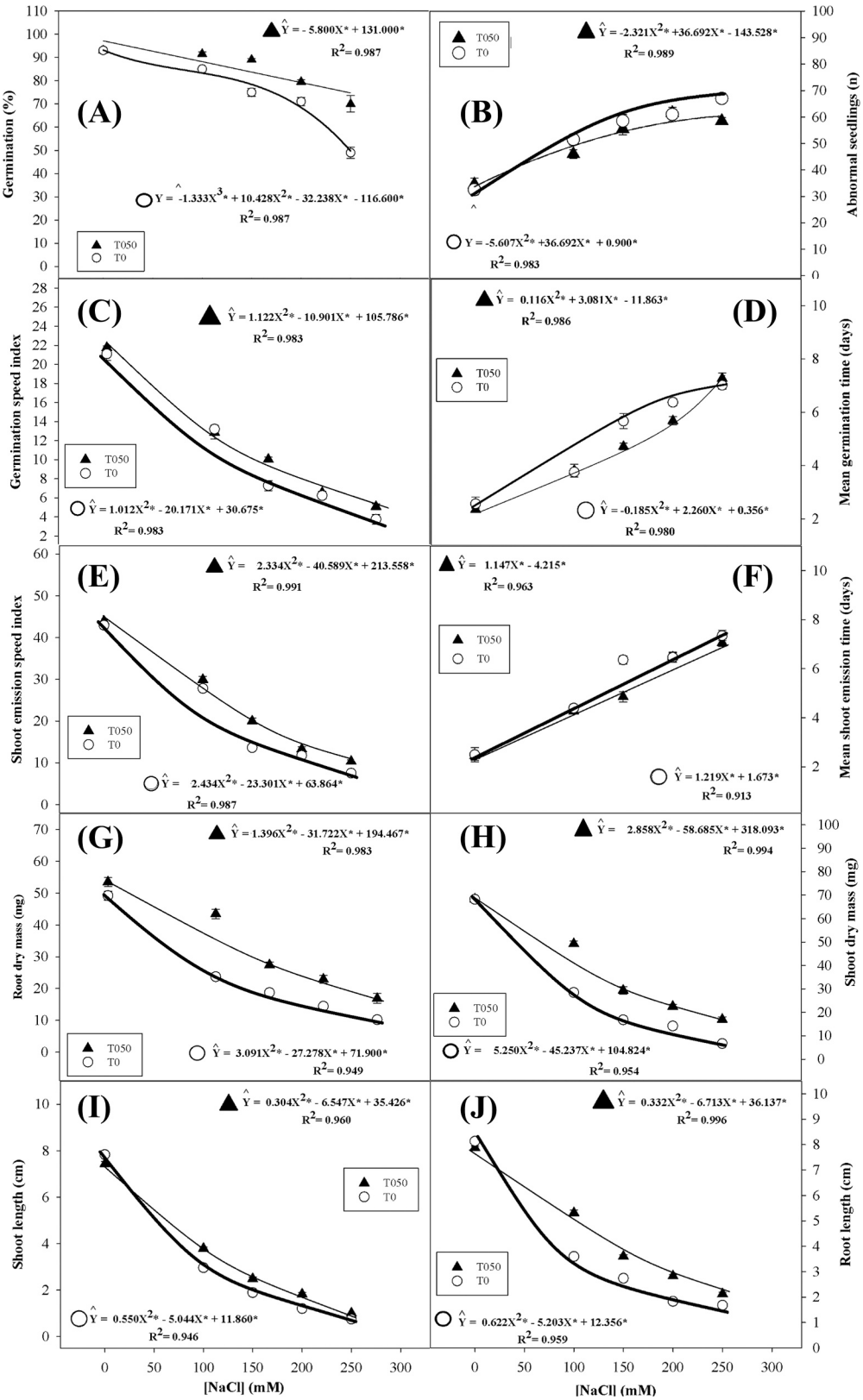

Fig. 1. NaCl screening regressions. Percentual of germination (A), number of abnormal seedlings (B), germination speed index (C), mean germination time (D), shoot emission speed index (E), mean shoot emission time (F), root dry mass (G), shoot dry mass (H), shoot length (I) and root length (J) of rice seeds and seedlings, primed with either 0 μg. mL^{-1} (O, thicker lines) or 0.50 μg. mL^{-1} (▲, thin lines) TM submitted to crescent concentrations of NaCl (0 – 250 mM). Circumflex accent (ˆ) over Y means the function was statistically significant. Regression points indicate means of 4 repetitions ± standard error; statistical analyses were represented by * as significant with $p < 0.05$.

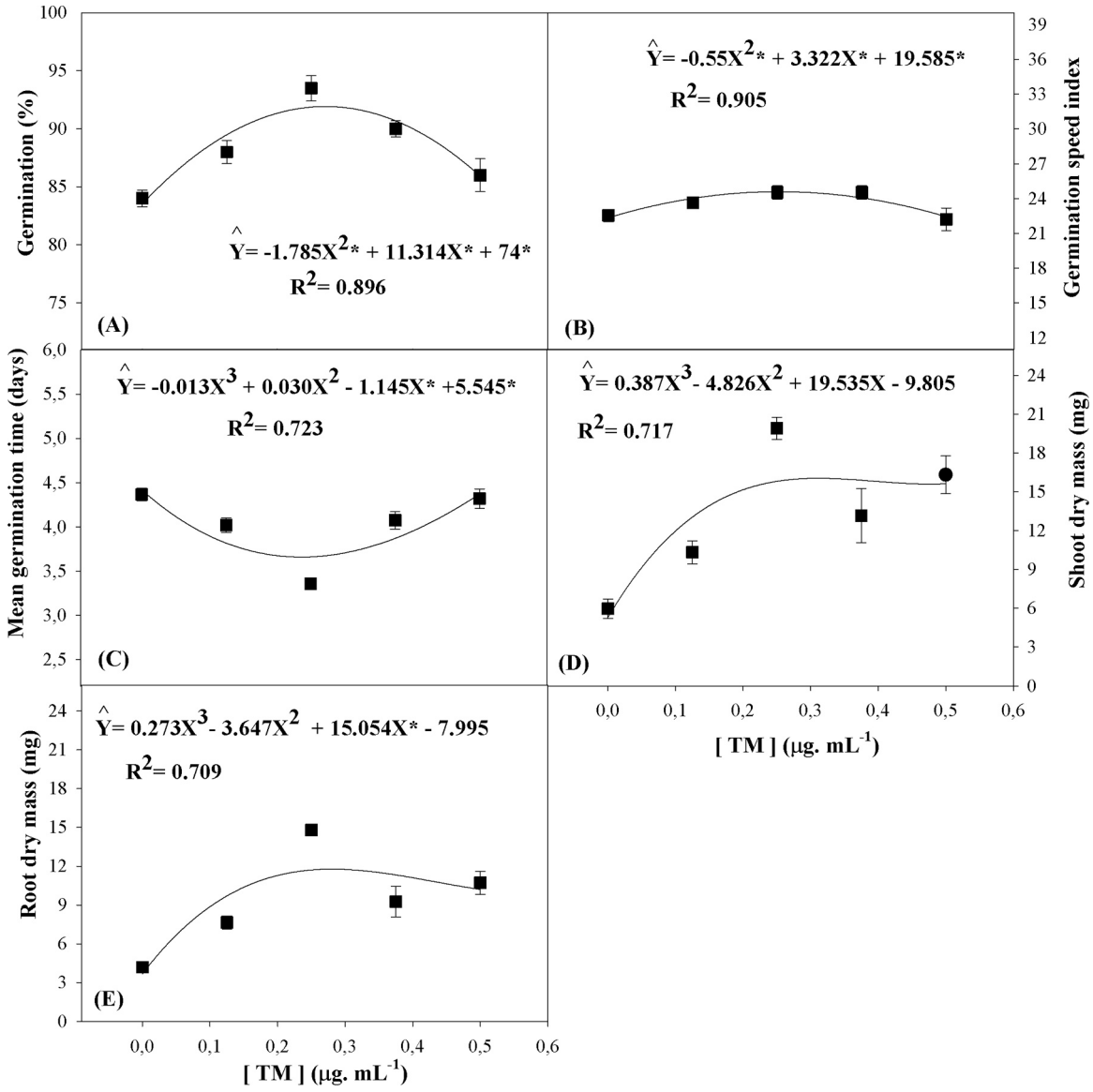

Fig. 2. Tunicamycin screening regressions. Percentual of germination (A), germination speed index (B), mean germination time (C), shoot dry mass (D) and root dry mass (E) of rice seeds and seedlings, primed with 0 µg. mL^{-1} to 0.50 µg. mL^{-1} (■, thin lines) TM under 150 mM NaCl. Regression points indicate means of 4 repetitions ± standard error; statistical analyses were represented by * as significant with $p < 0.05$.

factorial scheme (2 × 2), two concentrations of TM (0 and 0.25 µg. mL^{-1}) and two concentrations of NaCl (0 and 150 mM NaCl), generating thus four treatments: T0S0 (TM 0 µg.mL^{-1}, 0 mM NaCl), T025S0 (TM 0.25 µg.mL^{-1}, 0 mM NaCl), T0S150 (TM 0 µg.mL^{-1}, 150 mM NaCl), and T025S150 (TM 0.25 µg.mL^{-1}, 150 mM NaCl). Results were subjected to ANOVA analysis of variance, and the data means were compared by Tukey test ($p \leq 0.05$) using the SISVAR statistical program.

Metabolic data were normalized by log transformation and Range scaling. Mean values of the metabolites were compared using the T-tests to assess the effect within each treatment. Principal Component Analysis (PCA) was performed to identify the differences between the four treatments (T0S0, T025S0, T0S150, and T025S150) within each tissue (shoots and roots), and the most contributing metabolites were highlighted in the loading plots. To verify the effect of each TM treatment compared to their salt counterpart on the metabolic profiles, Orthogonal Partial Least Squares-Discriminant Analysis (OPLS-DA) was performed for shoots and roots of each variety, and variable importance in projections (VIP scores) were performed separately for each treatment, obtaining the principal discriminating metabolites. Hierarchical heatmaps were constructed by Euclidean distance based on a one-way analysis of variance (ANOVA).

3. Results

3.1. NaCl and TM screenings

Growing concentrations of NaCl from 100 to 250 mM decreased all germination parameters, such as the physiological ones (Fig. 1, A-J). However, TM priming displayed better performance than the control groups (T0). Aside from abnormal seedlings, exogenous TM priming significantly (with $p < 0.05$) improved germination percentage, GSI, SESI, RDM, SDM, SL, and RL, especially at 150 mM NaCl. Moreover, TM reduced mean germination time and mean shoot emergence time (Figs. 1D and 1F). Therefore, this experiment showed that 150 mM NaCl could allow the seedling establishment although it was severely repressed, but also had its parameters benefited by TM-priming, which is why it was chosen for further experiments. These data can be accessed in Supplementary Data (Tables S2 and S3). The germination rate of non-

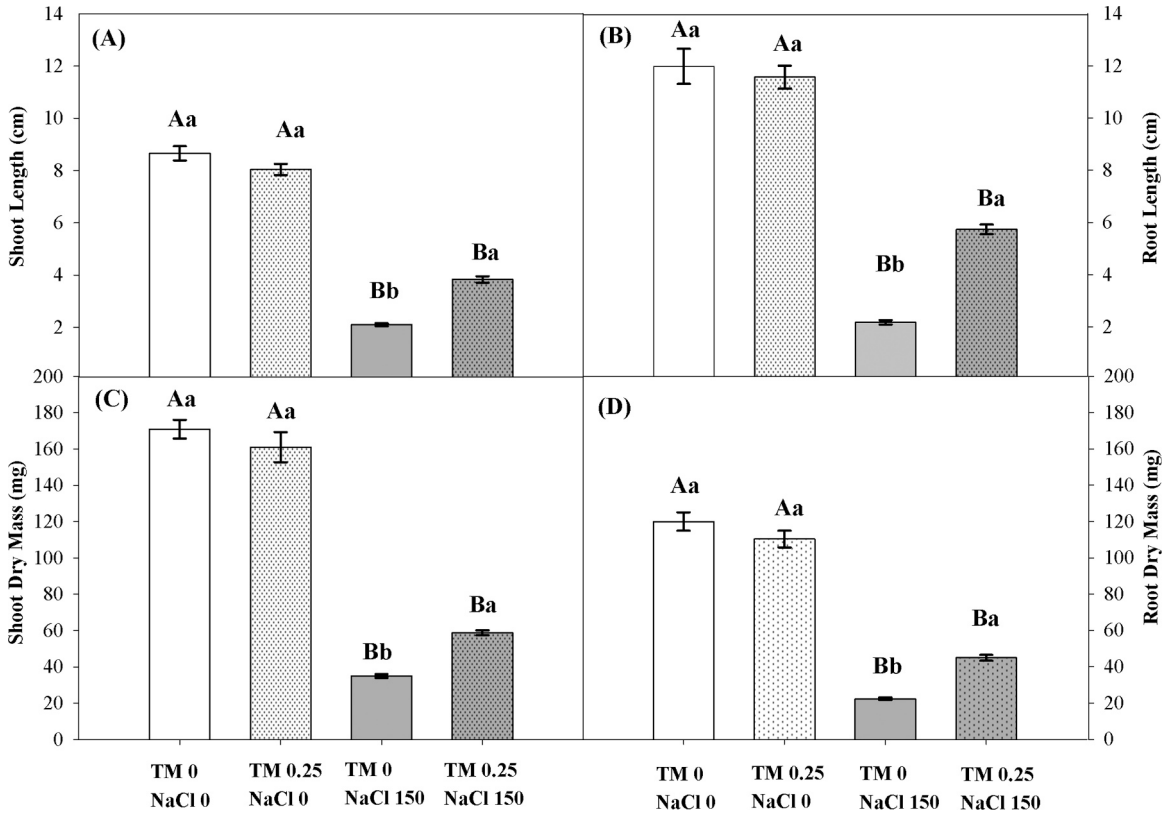

Fig. 3. Growth parameters of pre-treated seeds with tunicamycin (0 or 0.25 μg.mL) germinated in NaCl (0 or 150 mM) for 10 days. A) Shoot length; B) Shoot dry mass, C) Root length; D) Root dry mass. Different uppercase letters indicate statistical difference between distinct salt conditions within the same tunicamycin concentration, and lowercase letters indicate statistical difference among TM pre-treatments in the same NaCl concentration using Tukey test ($p < 0.05$). The bars represent the standard error (SE) of 4 biological repetitions.

primed seeds (TM0) displayed a quadratic behavior in function of NaCl concentrations, getting lower as the saline concentration increased (Fig. 1A). On the other hand, TM050 increased the germination rate in all NaCl treatments (Fig. 1A). Concerning GSI, both TM0 and TM050 displayed quadratic behaviors, in which T050 at 150 mM showed higher values than TM0 (Fig. 1C). MGT regressions revealed interesting behaviors: TM0 displayed a decreasing quadratic function as the NaCl concentrations grew, whereas TM050 showed an increasing quadratic one (Fig. 1D), with the last point (at 250 mM NaCl) being nearly at the same place as that one in TM0 function (Fig. 1D). SESI exhibited increasing quadratic behaviors, although it was higher in TM050 and 150 mM (Fig. 1E). MSET had the same pattern for both regressions. It showed increased linear behaviors as the NaCl concentrations augmented, with TM050 having a significantly lower value than this parameter at 150 mM NaCl, in contrast to T0 at the same saline point (Fig. 1F). Both root and shoot dry masses exhibited similar results, increasing quadratic functions for the TM treatments (Figs. 1G and 1H), with TM050 at 100 mM, showing much higher values (Figs. 1G and 1H). There were similar regressions for shoot and root lengths (Figs. 1I and 1J). It displayed quadratic behaviors in function of NaCl concentrations (Figs. 1I and 1J), but TM050 displayed higher scores, especially at 100 and 150 mM NaCl in RL (Fig. 1J).

For TM screening, we primed seeds with increasing TM concentrations and tested their germination under 150 mM NaCl. Although TM significantly increased all parameters in comparison to 0 TM, regressions showed that only five parameters achieved statistical significance (Table S4): germination percentage (Fig. 2A), GSI (Fig. 2B), MGT (Fig. 2C), SDM (Fig. 2D), and RDM (Fig. 2E). However, it is relevant to point out that, aside from GSI, 0.25 TM displayed the highest values in all those parameters (Fig. 2A – 2E). Regressions showed that TM concentrations induced a decreasing quadratic function of germination percentage, with the value at 0.25 TM being the highest and nearest the vortex of the equation (Fig. 2A). GSI regressions also displayed a quadratic function as TM concentrations increased, with the points 0.250 and 0.500 displaying very close values (Fig. 2B). MGT showed an increasing cubic function of regression, but only with the point at 0.250 TM showing the smallest value (Fig. 2C). In both shoot and root dry masses (Figs. 2D and 2E), regressions also showed decreasing cubic patterns, with 0.250 TM showing the highest values of these parameters (Figs. 2D and 2E). Therefore, 0.25 μg. mL^{-1} TM concentration was selected for further analyses as well.

3.2. Physiological parameters

In the absence of salinity, there was no significant difference between control and TM pre-treated seedlings (Fig. 3). However, salt stress decreased all physiological parameters in comparison to TM0. Conversely, TM-pre-treated ones alleviated the deleterious effects of salinity for all parameters. The increases of shoot and root, as well as dry masses of shoot and root lengths of TM pre-treated seedlings under salt treatment, were 45 %, 62 %, 40 %, and 50 %, respectively, compared to control seedlings under salinity (Fig. 3A-D, and Supplementary Figure S1).

3.3. Electrolyte leakage and osmotic potential

Salinity reduced the osmotic potential of shoots, and TM priming increased it by 25 % (Fig. 4A). Furthermore, NaCl treatment increased electrolyte leakage in the shoots and roots of seedlings. However, TM priming significantly increased these effects in shoots and roots, 32 % and 25 %, compared to the absence of priming (Figs. 4B and 4C).

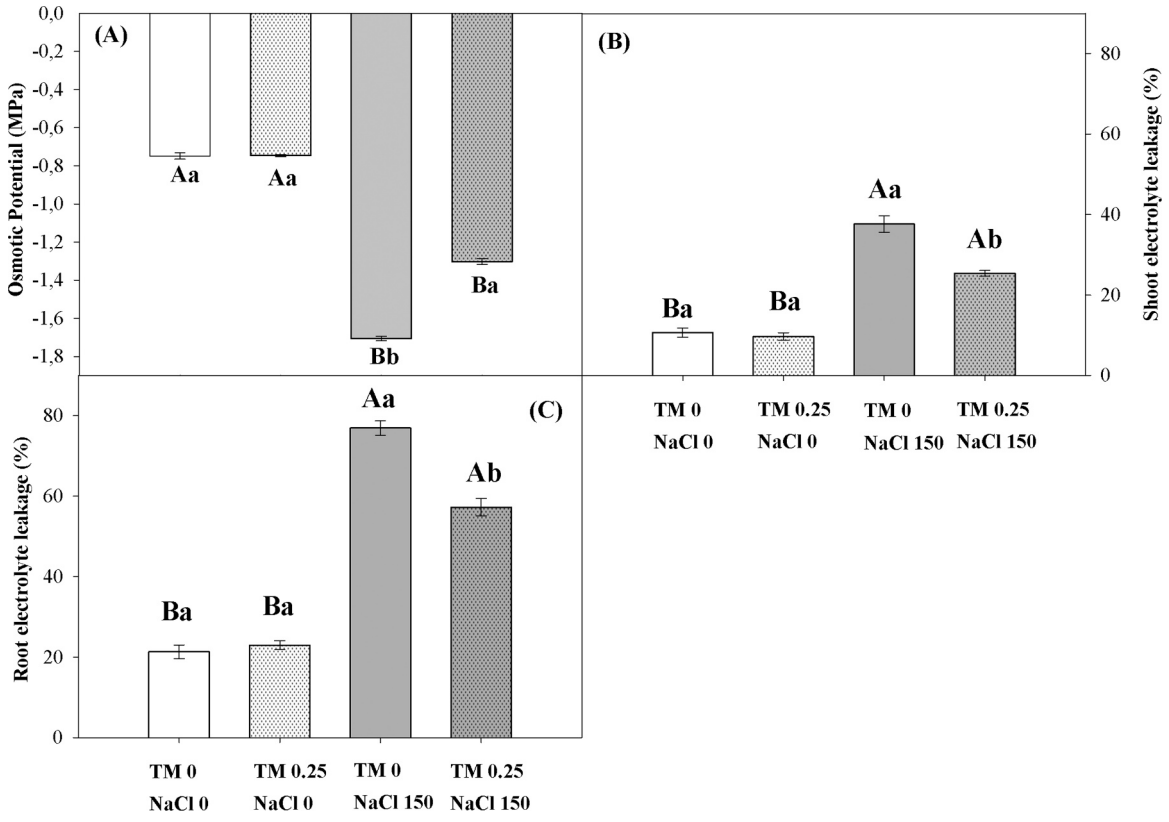

Fig. 4. Osmotic potential (A), and electrolyte leakage of shoots (B), and roots (C) of seedlings pre-treated with tunicamycin (0 or 0.25 μg.mL) germinated in NaCl (0 or 150 mM) for 10 days. Different uppercase letters indicate statistical difference between distinct salt conditions within the same tunicamycin concentration, and lowercase letters indicate statistical difference among TM pre-treatments in the same NaCl concentration using Tukey test ($p < 0.05$). The bars represent the standard error (SE) of 4 biological repetitions.

3.4. Photosynthetic pigments

Salt stress decreased all photosynthetic pigment contents, but the TM pre-treatment ameliorated this effect compared to non-pretreated shoots. There were increases of 61 % in chlorophyll A content (Fig. 5A), 30 % in chlorophyll B content (Fig. 5B), 31 % in total chlorophyll content (Fig. 5C), and 26 % in carotenoid content (Fig. 5D) promoted by seed pre-treatment.

3.5. Inorganic ion contents (Na^+, K^+, and Cl^-)

The Na^+ content in 150 mM NaCl-treated seedlings increased in shoots and roots. However, TM-primed reduced Na^+ levels by 36 % in shoots (Fig. 6A) and 22 % in roots (Fig. 6B). In contrast, K^+ content in shoots was not modified by salinity between TM-primed groups (T025S0 and T025S150). Comparing both stressed treatments, TM induced an increase of this ion by 33 % compared to T0S150 shoots (Fig. 6C). In roots, levels of this ion (K^+) decreased with the salt treatment (Fig. 6D). Nevertheless, TM-conditioning alleviated this condition, expressing an increase of 29 % (Fig. 6C) in shoots and 24 % (Fig. 6D) in roots, compared to TM0. Concerning the K^+/Na^+ ratio, NaCl-treated seedlings underwent a decrease in this parameter in both shoots and roots. Despite that, the TM-primed group revealed an elevation of 50 % in shoots (Fig. 6E) and 44 % in roots, respectively (Fig. 6F). Similarly to Na^+, Cl^- content significantly increased in shoots and roots in the presence of 150 mM NaCl. Nevertheless, TM-pre-treated seedlings under salt stress exhibited a reduction in Cl^- of 26 % in shoots (Fig. 6G) and 24 % in roots (Fig. 6H).

3.6. Detection of Na^+ by confocal microscopy

Confocal microscopy fluorescence revealed the Na^+ dynamics in leaf tissues showed higher Na^+ accumulation in the shoots, especially in the epidermal cells and within such cells (Fig. 7A), and in the root hairs (Fig. 7B) of NaCl-treated seedlings. However, seedlings from primed seeds under salinity decreased fluorescence emission, evidenced by the lower intensity green emission for shoots (Fig. 7A) and roots (Fig. 7B). The intensity of fluorescence in shoots (Fig. 7C) and roots (Fig. 7D) was measured using Zen software. It showed lower intensity in both tissues in TM-treated seedlings under salt stress, which confirmed that TM-priming reduced Na^+ content in the apoplast.

3.7. Reactive oxygen species (H_2O_2 and $\cdot O_2^-$) contents and lipid peroxidation

As expected, salt stress increased H_2O_2 content in NaCl-treated seedlings compared to control groups. Interestingly, at 150 mM NaCl, TM-pre-treated seedlings showed a reduction of this ROS of 25 % in shoots (Fig. 8A) and 32 % in roots (Fig. 8B). Similarly, salinity also increased $\cdot O_2^-$ content in shoots and roots (Fig. 8E and Fig. 8F). However, only TM-pre-treated shoots significantly reduced their production, with a decrease of 30 % when compared to TM0 seedlings under salt stress (Fig. 8E). The increased H_2O_2 and $\cdot O_2^-$ may induce malondialdehyde (MDA) production (a marker of lipid peroxidation). NaCl stress increased MDA content in both shoots and roots of salt-treated rice seedlings (Figs. 8C and 8D). On the other hand, TM-pre-treated seedlings managed the decrease of this production compared to those non-pre-treated ones under 150 mM NaCl, presenting a reduction of 33 % in shoots (Fig. 8C) and 25 % in roots (Fig. 8D).

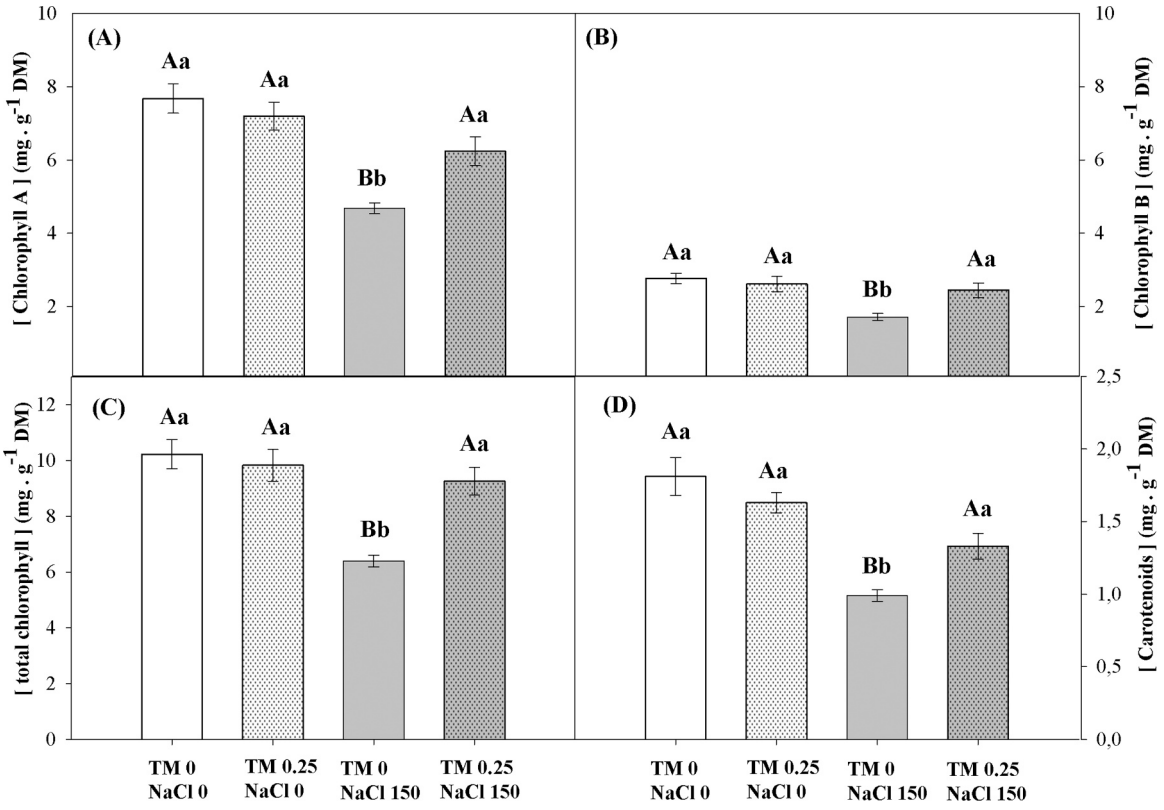

Fig. 5. Photosynthetic pigment contents of pre-treated seeds with tunicamycin (0 or 0.25 μg.mL) and germinated in NaCl (0 or 150 mM) for 10 days. A) chlorophyll A content, B) chlorophyll B content, C) total chlorophyll content, and D) carotenoid content. Different uppercase letters indicate statistical difference between distinct salt conditions within the same tunicamycin concentration, and lowercase letters indicate statistical difference among TM pre-treatments in the same NaCl concentration using Tukey test ($p < 0.05$). The bars represent the standard error (SE) of 4 biological repetitions.

3.8. Antioxidant enzyme activities (SOD, CAT, APX and GPOD)

Salt stress increased CAT activity in both shoots and roots of rice seedlings (Figs. 9A and 9B). However, TM-conditioning significantly augmented this enzyme activity in shoots and roots by 25 % (Fig. 9A) and 31 % (Fig. 9B), respectively, compared to TM0. For Ascorbate peroxidase (APX), salt stress increased APX activity in both stressed treatments (Figs. 9C and 9D, respectively). Interestingly, TM-pre-treatment did not cause any significant variation in this enzyme activity. Once $\cdot O_2^-$ is the substract for SOD, it is assumed that this enzyme has its activity increased by salinity as well. As a matter of fact, NaCl augmented SOD activity in both stressed treatments in shoots and roots (Figs. 9E and 9F). TM-priming induced a significant increase in SOD activity of 27 % in shoots (Fig. 9E) and 30 % in roots (Fig. 9F), respectively. H_2O_2 is also substract for GPOD, so one can assume this enzyme has its activity augmented in the presence of NaCl. Salt stress did increase its activity in both NaCl treatments (Figs. 9G and 9H). On the other hand, TM-primed seedlings under 150 mM NaCl displayed significantly increased activities in both shoots and roots, respectively, 26 % (Fig. 9G) and 30 % (Fig. 9H).

3.9. Gene expression analysis

In the absence of salt, TM promoted a decrease of *OsIRE1* only in the shoot, also in the absence of TM, *OsIRE1* was decreased by salinity (Fig. 10A). Conversely, there were no significative changes of *OsIRE1* expression induced by TM or salinity in roots, nor *OsbZIP50* (*Atb*ZIP60 ortholog) in both shoots and roots (Fig. 10B-D). On the other hand, in the presence of salt, the TM priming promoted a remarkable increase of *OsIRE1* and *OsbZIP50* in booth shoots and roots in comparison to salt without TM priming, it was higher in roots suggestion a much strong UPR activation in roots (Fig. 10A-D). Similarly, the expression of *OsbZIP60* (*Atb*ZIP28 ortholog) increased in shoots of primed seed grown under salinity, however it decreased in roots (Table S5). Although we could not detect the amplification in all treatments, the expressions of *OsBiP4* and *OsBiP5* were high in shoots and roots of primed seeds grown under salinity, respectively. However, we could not find consistency in the expressions of *OsNHX1,* the expression of *OsSOS1* seems to increase under salinity, in comparison to control plants (Table S5).

3.10. Metabolomic profiling analysis

A total of 40 metabolites were identified among treatments, of which 15 were amino acids, 10 were organic acids, 11 were carbohydrates, and 4 belonged to other classes (Table 1). The classification was based on the KEGG ID or PubChem, the retention times, and mass fragmentation pattern. Among them, 36 were found in both shoots and roots, whereas 6 were exclusive to roots: the sugars mannose and sorbitol, lactic acid dimer (organic acid), N-acetyl-serine and lysine (amino acids), and urea (other compound).

To assess the differences between TM-untreated and TM-treated, multivariate analyses of the principal component (PC) of the GC-MS dataset from seedling shoots and roots were performed. Concerning shoots, PC1 and PC2 accounted for 29.8 % and 11.3 %, respectively (Fig. 11A). The plot showed a complete separation of groups based on NaCl concentrations: 0 mM NaCl treatments were set apart from 150 mM, mainly influenced by PC1 component. There were overlaps between treatments with the same TM concentrations (Fig. 11A). The top four positive contributions to PC1 in shoots were glyceric acid, phenylalanine, salicylic acid, and erythrose, while to PC2 were galactose, serine, asparagine, and glycolic acid (Fig. 11B, Table S7).

The Heatmaps detailing positive or negative modulation of

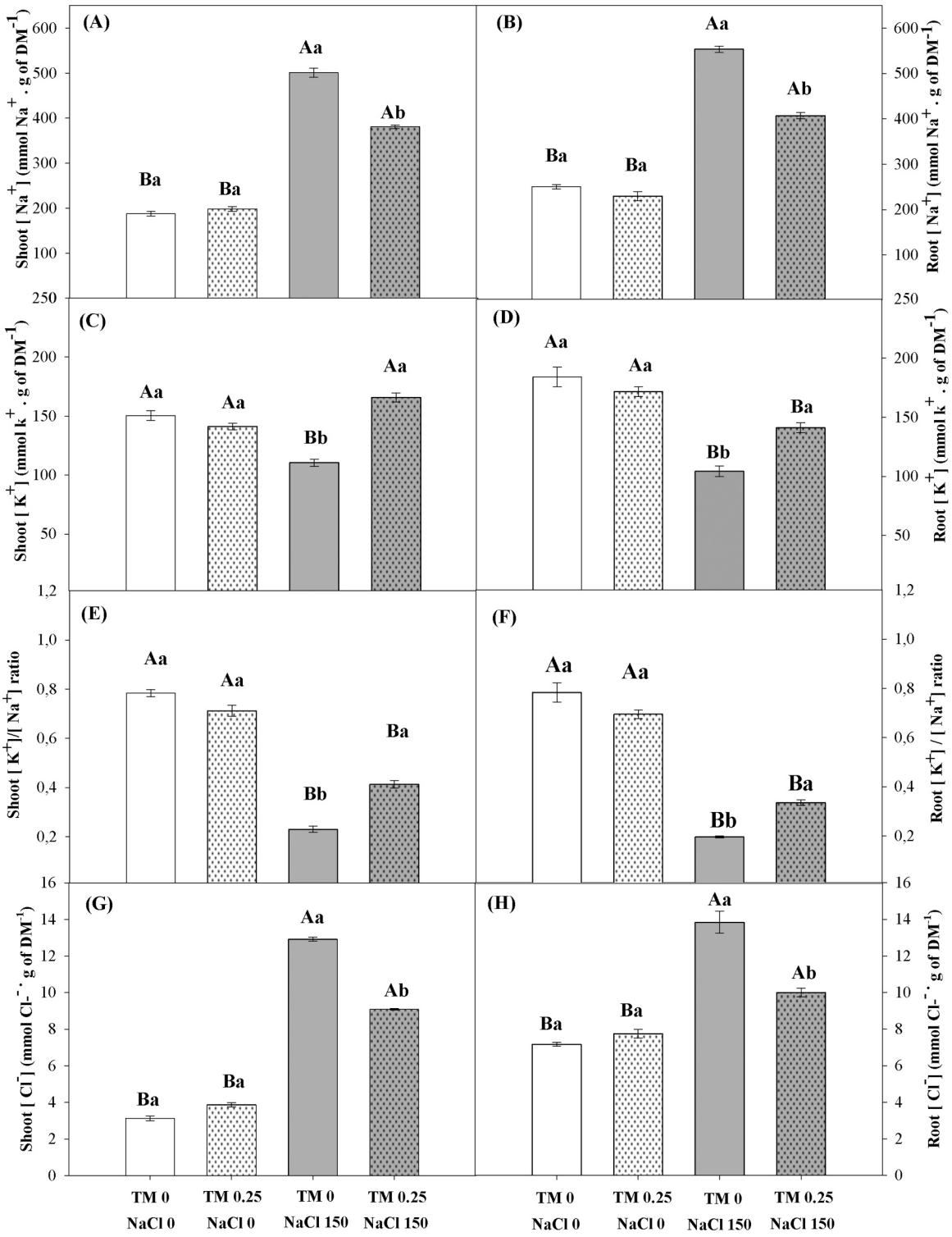

Fig. 6. Inorganic ion contents of pre-treated seeds with tunicamycin (0 or 0.25 μg.mL) and germinated in NaCl (0 or 150 mM) for 10 days. A) Shoot K^+, B) shoot Na^+, C) root K^+, D) root Na^+, E) shoot K^+/Na^+ ratio, F) shoot K^+/Na^+ ratio, G) Shoot Cl^-, and H) Root Cl^- content. Different uppercase letters indicate statistical difference between distinct salt conditions within the same tunicamycin concentration, and lowercase letters indicate statistical difference among TM pre-treatments in the same NaCl concentration using Tukey test ($p < 0.05$). The bars represent the standard error (SE) of 4 biological repetitions.

metabolites were generated comprising both TM (0 and 0.25 μg. mL^{-1}) and NaCl (0 and 150 mM) concentrations, similarly to the PCA. Shoot heatmap analysis displayed a division between 0 mM NaCl and 150 mM NaCl treatments (Fig. 11C). In general, metabolites with lower abundance in the absence of salt (T0S0 and T025S0) became positively modulated by salinity, and vice versa (Boxes 1, 2, and 3). Metabolites with statistical differences ($p < 0.05$) were identified among the treatments (Supplementary table S7) and plotted in a heatmap as circles and triangles. In salt absence, TM pre-treatment positively modulated putrescine, valine, lactic acid, isoleucine, threonine, phenylalanine, and maltotriose compared to control (circles in T025S0 column). Comparing control versus salt treatment (T0S0 x T0S150), 19 metabolites were

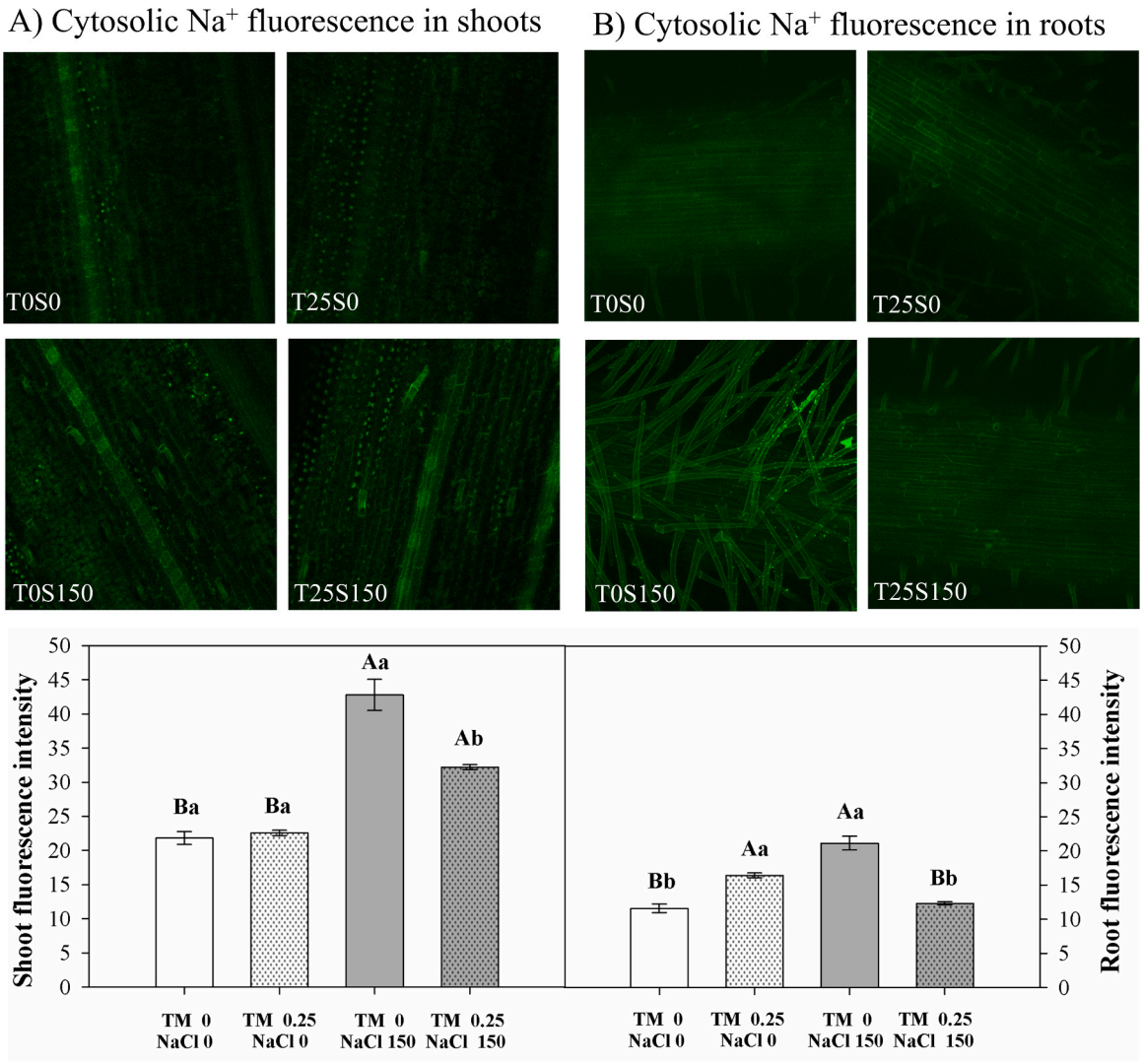

Fig. 7. NaTRIUM Green-2AM Fluorescence in pre-treated seedlings with tunicamycin (0 or 0.25 μg.mL) and germinated in NaCl (0 or 150 mM) for 10 days, in shoots (A) and roots (B), the intensities of each fluorescence were estimated. Different uppercase letters indicate statistical difference between distinct salt conditions within the same tunicamycin concentration, and lowercase letters indicate statistical difference among TM pre-treatments in the same NaCl concentration using Tukey test ($p < 0.05$). The bars represent the standard error (SE) of 4 biological repetitions.

significantly down-modulated under salinity, the amino acids glycine, isoleucine, 4-aminobutyric acid, threonine, phenylalanine, histidine, and asparagine; the carbohydrates maltotriose, myo-inositol, erythrose, glucose, and galactose; the organic acids succinic acid, oxalic acid, glyceric acid, glycolic acid, and pyruvic acid; and the secondary metabolites (others) quinic acid, salicylic acid (triangles in T0S0 column). Otherwise five metabolites were up-modulated by salinity (triangles in T0S150 column), glutamic acid, O-acetyl-serine, and beta-alanine; maltose, and putrescine. Regarding T025S150, only three metabolites were positively modulated compared to T025S0 (see circles in T25S150 colum), O-acetylserine, beta-alanine, and maltose. Comparing T025S150 and T0S150, only oxalic acid was significantly higher (circle in T025S150 column), whereas five metabolites had higher concentrations in T0S150 (see circles in T0150, glutamic acid, serine, and threonine, maltose, and glycolic acid.

In roots, PC1 and PC2 accounted for 27.5 % and 12.5 %, respectively (Fig. 12A). Similarly to shoots, the plot showed a complete separation of groups based on NaCl concentrations, induced by the PC1 component. Curiously, there were overlaps between treatments with the same TM concentrations, mainly influenced by the PC1 component. The top four positive contributions to PC1 in roots were citric acid, putrescine, O-acetylserine, and glutamic acid, and to PC2 were glucose, phenylalanine, threonine, and putrescine (Fig. 11B, Table S7).

Heatmaps detailing positive or negative modulation of root metabolites were generated comprising both TM (0 and 0.25 μg. mL^{-1}) and NaCl (0 and 150 mM) concentrations, similarly to the PCA (Fig. 12C and Supplementary Table S9). Comparing T0S0 roots and T0S150, 15 metabolites were significantly downregulated by salinity (triangles in T0S0 column, Box 1): the amino acids asparagine, glycine, and histidine; the organic acids citric acid, lactic acid, lactic acid dimer, and pyruvic acid; the sugars galactose, glucose, mannose, fructose, maltotriose, and myo-inositol; and secondary metabolites (others) quinic acid and urea. Conversely, 18 were up-modulated by salinity (triangles in T0S150 column, box 2): the amino acids phenylalanine, threonine, 4-aminobutyric acid, lysine, glutamic acid, O-acetylserine, beta-alanine, alanine, N-acetylserine, valine, isoleucine, and serine; the sugars raffinose, sucrose, maltose, sorbitol; and the others, phosphoric acid and putrescine. Comparing both NaCl-stressed treatments, T025S150 and T0S150, 14 metabolites were positively modulated (circles in T025S150 column, Box 3), the amino acids asparagine, glycine, histidine, isoleucine, serine,

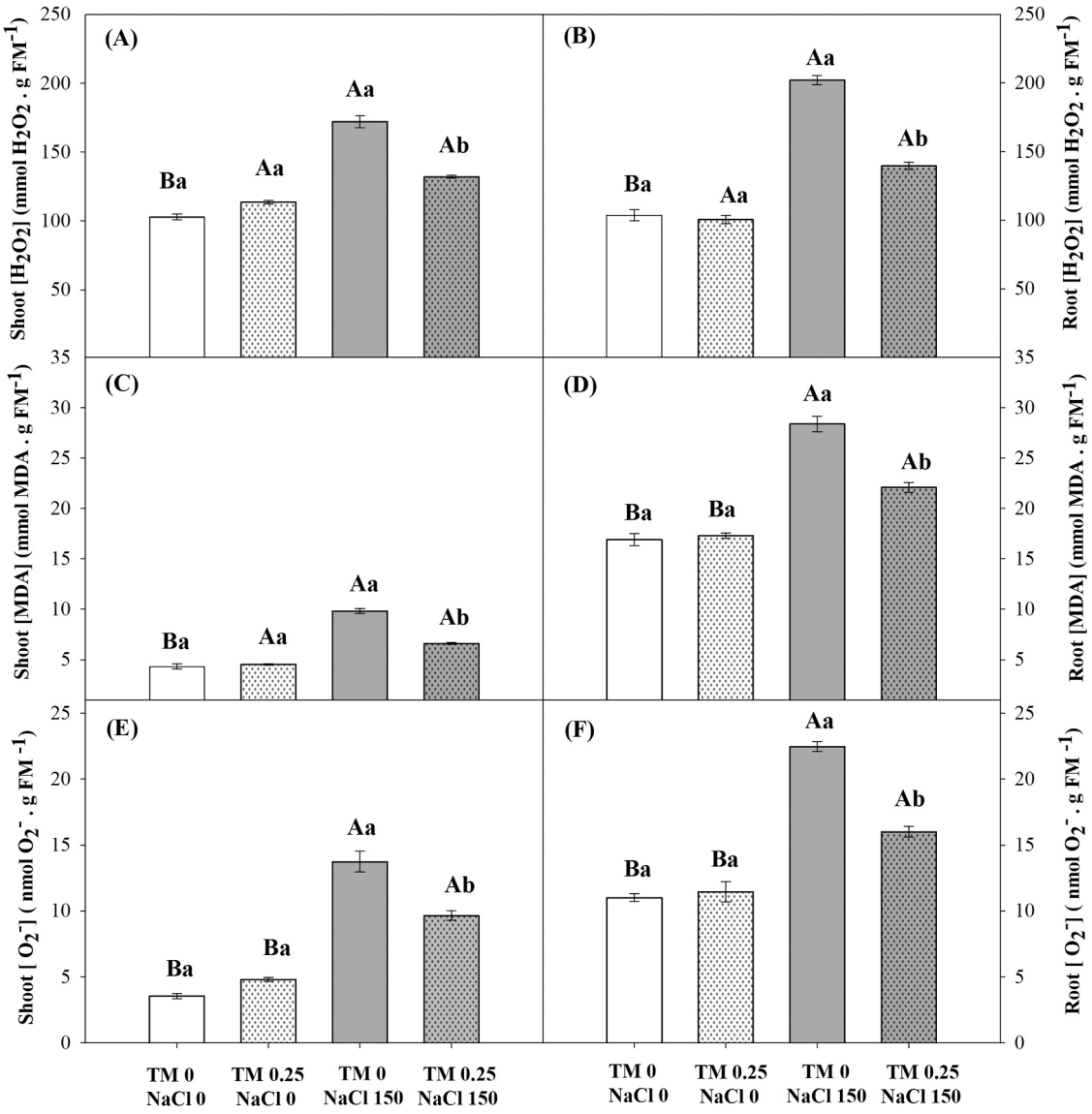

Fig. 8. Reactive oxygen species and lipid peroxidation of pre-treated seeds with tunicamycin (0 or 0.25 μg.mL) and germinated in NaCl (0 or 150 mM) for 10 days. A) shoot H_2O_2 content, B) root H_2O_2 content, C), shoot MDA content, D) root MDA content, E) shoot $\cdot O_2^-$ content, and F) root $\cdot O_2^-$ content. Different uppercase letters indicate statistical difference between distinct salt conditions within the same tunicamycin concentration, and lowercase letters indicate statistical difference among TM pre-treatments in the same NaCl concentration using Tukey test ($p < 0.05$). The bars represent the standard error (SE) of 4 biological repetitions.

and phenylalanine; the sugars galactose, mannose, sorbitol, glucose and myo-inositol; and the secondary metabolites (others) putrescine and urea, whereas only lysine was higher in T0S150.

Based on metabolic profiles, we performed the orthogonal partial least squares discriminant analyses (OPLS-DA) to find the positive and negative potential biomarkers of TM and NaCl presence (Fig. 13). Analyzing T0S150 shoots compared to T0S0, the top three discriminant metabolites were maltose, beta-alanine, and O-acetylserine, whereas the most negative was maltotriose (Fig. 12A). Concerning T025S150 shoots versus T025S0, the top three positive metabolites were O-acetylserine, beta-alanine, and maltose, whilst the most negative one was threonine (Fig. 13B). In roots, observing OPLS-DA S-plots from T0_S150 compared to T0S0, the top three most positive metabolites were putrescine, sorbitol, and glutamic acid, whereas the most negative one was asparagine (Fig. 13C). Analyzing T025S150 compared to T025S0, the top three most positive metabolites were glutamic acid, raffinose, and O-acetylserine, whilst the most negative one was lactic acid dimer (Fig. 13D).

4. Discussion

4.1. TM seed priming improves seed germination traits under salinity

To survive in a stressful environment, plants have to develop approaches and mechanisms to cope with environmental challenges, such as biotic factors (viruses and fungi) and abiotic ones (salinity); among some strategies, we can mention a more efficient antioxidant system and more cellular energy (ATP) production (Georgieva and Vassileva, 2023). For instance, both osmotic and ionic components triggered by salinity not only impair germination and physiological traits, but also several molecular processes, such as photosynthesis, water status, and ion balance (Ganie et al., 2024). But also generate secondary stresses, such as oxidative, ionic, and ER stresses, which can lead to inhibition of growth and crop yield (Chele et al., 2021). Indeed, in this current work, the increase of NaCl promoted a decrease in germination percentage, GSI, and SEI, as well as increased the GT, and MSET which compromised RDM, SDM, SK, and RL of seedlings after 10 DAT (Fig. 1).

Given that rice plants present sensitivity to salinity in this stage (Liu

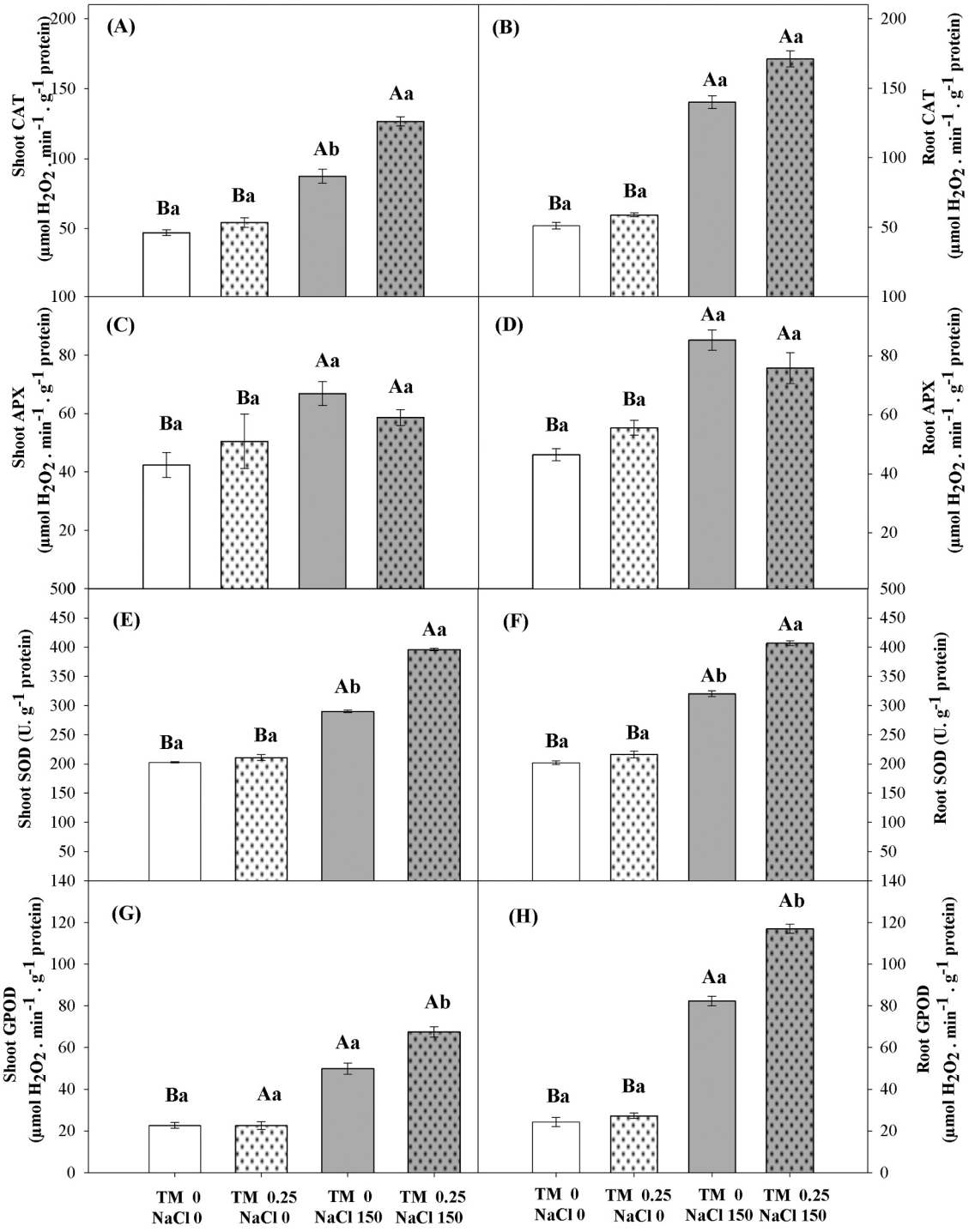

Fig. 9. Antioxidant enzymatic system evaluation, of pre-treated seeds with tunicamycin (0 or 0.25 µg.mL) and germinated in NaCl (0 or 150 mM) for 10 days. A) Catalase in shoots, B) catalase in roots, C) ascorbate peroxidase in shoots, D) ascorbate peroxidase in roots, E) superoxide dismutase in shoots, F) superoxide dismutase in roots, G) guaiacol peroxidase in shoots, and H) guaiacol peroxidase in roots. Different uppercase letters indicate statistical difference between distinct salt conditions within the same tunicamycin concentration, and lowercase letters indicate statistical difference among TM pre-treatments in the same NaCl concentration using Tukey test ($p < 0.05$). The bars represent the standard error (SE) of 4 biological repetitions.

et al., 2022b), strategies that alleviate the deleterious effects of NaCl in plants are necessary (Çakır Aydemir et al., 2020). In this way, seed priming exposes plants to a mild dose of stress, enabling them to stand more severe conditions (Aswathi et al., 2022). This methodology not only minimizes salinity toxicity but also strengthens the defense system of crops. Here, the hydration level within the seeds was controlled by applying pre-sowing treatments, allowing specific pre-germinative metabolic processes to occur and preventing radical emergence (Khan et al., 2022b). It also helps in DNA replication responses, antioxidant function, more ATP availability, and encouraged protein biosynthesis, restoring cellular bio-membranes, and improving antioxidant enzymes (Mansour et al., 2019). Several studies corroborate our work with seed priming, priming rice seeds with a mixture of 100 mM NaCl, and other salts ($CaCl_2$, and KCl) not only did increase root and shoot dry masses, but also decreased Na^+ content in leaves and roots, and raised relative water content in primed seeds (Hidayah et al., 2022), which is in

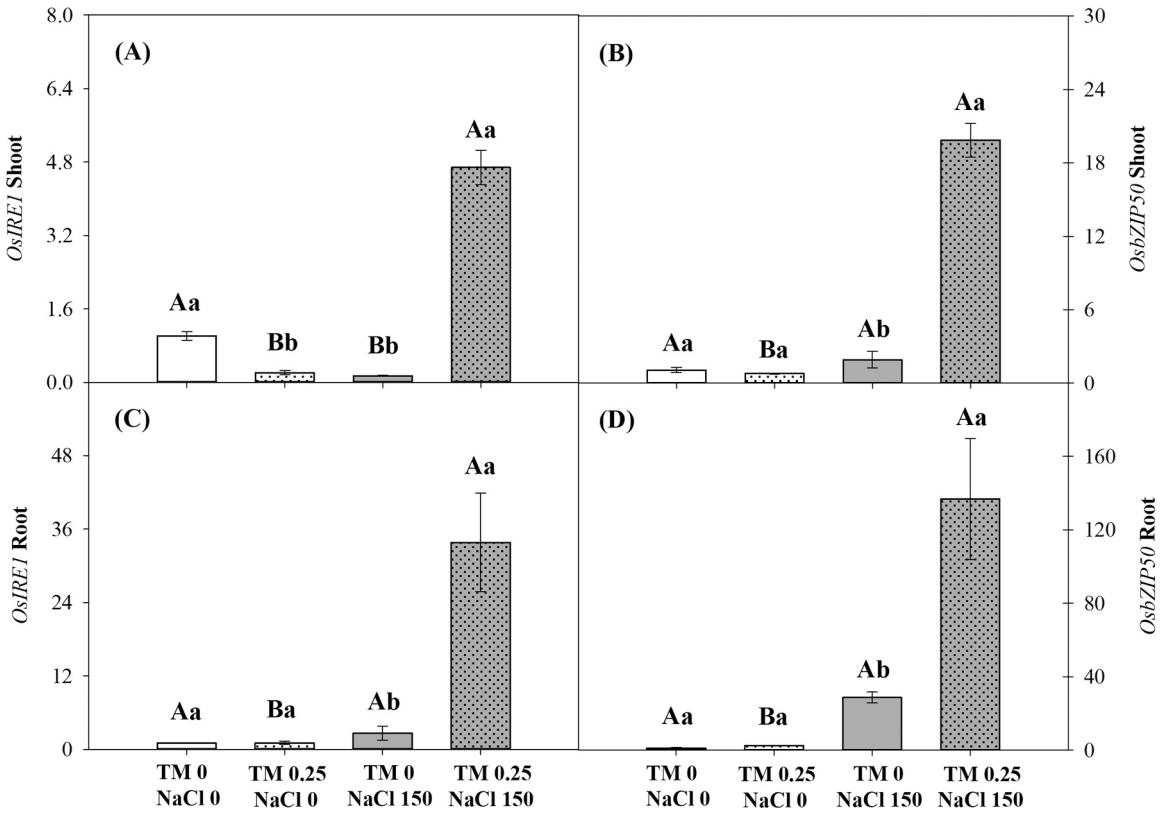

Fig. 10. Relative gene expressions of pre-treated seeds with tunicamycin (0 or 0.25 μg.mL) and germinated in NaCl (0 or 150 mM) for 10 days. A-B) *OsIRE1* and *OsbZIP50* in shoots C-D) *OsIRE1* and *OsbZIP50*. Gene expressions were normalized using *OsUBQ* as a reference gene and the values expressed as $2^{-\Delta\ \Delta CT}$. The columns indicate the mean of three biological replicates and the bars indicate the standard deviation. Different uppercase letters indicate statistical difference between distinct salt conditions within the same tunicamycin concentration, and lowercase letters indicate statistical difference among TM pre-treatments in the same NaCl concentration using Tukey test ($p < 0.05$). The bars represent the standard error (SE) of 3 biological repetitions.

accordance with our work. Also, our results were corroborated by by salicylic acid (SA) priming, the AS increased GSI and germination potential by inducing SOD, CAT, and APX activities, therefore reducing ROS contents, and by increasing gibberellin production (Liu et al., 2022b).

It is known that salt stress induces an overaccumulation of unfolded proteins, which leads to endoplasmic reticulum (ER) stress (Park and Park, 2019b; Reyes-Impellizzeri and Moreno, 2021). Since more than one-third of plant cell proteins are synthesized and folded in this organelle, it is vital that the repair and degradation mechanisms should work well, as several N-glycosylated proteins are produced there, and most of them are enzymes, which might be associated with acclimation and tolerance (Strasser et al., 2021). Furthermore, there is an upregulation of UPR and ER quality control genes during priming maintained after recovery, allowing salt-primed plants to exhibit better growth in response to future salt exposure (Tian et al., 2019). Here, these gene expressions were much higher in roots than shoots, probably because it is in contact with salt and may contributed to much higher accumulation of metabolites in roots than shoots under salt. Thus, it corroborated our thoughts that TM, an inductor ER response, could act as a priming to induce salt acclimation in rice.

Exogenous TM causes ER stress, leading to an ER response (Manghwar and Li, 2022; Astani et al., 2022). Indeed, this response is crucial to cell survival since the time of exposure increases ER stress and promotes a decrease of specific genes, impairment of metabolic pathways, and seedling growth (Lima et al., 2022). However, lower concentrations of TM (0.5 $\mu g.L^{-1}$) promote biomass maintenance and seedling length associated with high ER gene expression (Cavalcante et al., 2023). Here we noticed that seed TM priming maintained germination traits and seedling growth under salt stress (Fig. 1). Likewise, these results were corroborated when we tested different doses of TM, in which 0.25 $\mu g.L^{-1}$ provided the best impacts (Fig. 2). Thus, to explore how TM seed priming can prepare seedlings for severe salt conditions, we set a new experimental strategy using a combination of priming and unprimed seeds in the absence and presence of NaCl.

4.2. TM seed priming induce ER responses to mitigates negative effects of salinity in seedlings

Besides seed germination indexes and growth parameters previously discussed, salinity severely impacted osmotic potential, chlorophyll and carotenoid contents as well as increased cell damage by electrolyte leakage (Figs. 1–5). However, TM seed priming promoted the maintenance of all physiological and biochemical parameters, which is mainly due to decreased Na^+ contents in both shoots and roots, promoted by TM (Fig. 6), which led to less production of ROS, and allowed the increase in these parameters. Such results are in accordance with previous studies of different priming agents. KNO_3 seed priming not only reduced electrolyte leakage but also increased the total chlorophyll content of rice seedlings under 150 mM NaCl (Theerakulpisut et al., 2016). In another work, priming seeds with NaCl decreased electrolyte leakage and damage to the photosynthetic apparatus, as well as promoted higher root growth and ABA levels, protecting against drought stress (Rossatto et al., 2023).

Here, TM-priming not only increased total chlorophyll content, but also augmented carotenoid content, which might have led to more efficient photosynthetic processes and, consequently, higher initial growth, biomass, and lengths of TM-conditioned seedlings under salt stress. Certainly, photosynthesis is a vital process for plants, and most chloroplast-located proteins are produced in the ER and then

Table 1
List of total metabolites found in rice seedlings.

Metabolite	Compound Type	Retention Time (MIN)	Compound ID	Database
4-Aminobutyric acid	Amino acid	16.57	C00334	KEGG
Alanine	Amino acid	8.39	C00041	KEGG
Asparagine	Amino acid	18.78	C00152	KEGG
beta - Alanine	Amino acid	14.91	C00099	KEGG
Glutamic acid	Amino acid	17.95	C00025	KEGG
Glycine	Amino acid	12.78	C00037	KEGG
Histidine	Amino acid	22.12	C00135	KEGG
Isoleucine	Amino acid	12.54	C00407	KEGG
Lysine	Amino acid	22.06	C00047	KEGG
N-acetyl-serine	Amino acid	17.58	65249	PubChem
O-acetyl-serine	Amino acid	14.94	C00979	KEGG
Threonine	Amino acid	14.30	C00188	KEGG
Valine	Amino acid	10.98	C00183	KEGG
Citric acid	Organic acid	20.81	C00158	KEGG
Glyceric acid	Organic acid	13.28	C00258	KEGG
Glycolic acid	Organic acid	7.73	C00160	KEGG
Lactic acid	Organic acid	7.36	C00186	KEGG
Lactic acid dimer	Organic acid	12.63	10034905	PubChem
Malic acid	Organic acid	15.98	C00149	KEGG
Oxalic acid	Organic acid	9.14	C00209	KEGG
Phosphoric acid	Organic acid	12.21	C00009	KEGG
Pyruvic acid	Organic acid	7.10	C00022	KEGG
Succinic acid	Organic acid	12.86	C00042	KEGG
Fructose	Sugar	21.61	C00095	KEGG
Galactose	Sugar	22.19	C00124	KEGG
Glucose	Sugar	21.94	C00031	KEGG
Myo-inositol	Sugar	24.23	C00137	KEGG
Maltose	Sugar	30.93	C00208	KEGG
Maltotriose	Sugar	34.10	C01835	KEGG
Mannose	Sugar	21.87	C00159	KEGG
Raffinose	Sugar	32.18	C00492	KEGG
Sorbitol	Sugar	21.73	C00764	KEGG
Sucrose	Sugar	30.03	C00089	KEGG
Putrescine	Others	17.42	C00134	KEGG
Quinic acid	Others	21.41	C00296	KEGG
Salicylic acid	Others	16.29	C00805	KEGG
Urea	Others	11.57	C00086	KEGG

transported to chloroplasts via the secretory pathway, such as carbonic anhydrase (Jiao et al., 2020). Since salinity strongly impairs photosynthesis, it is interesting that TM conditioning alleviates this condition by inducing ER and downstream responses. Although other ER genes remain to be evaluated, the downstream responses were observed here, which included the increased expression of *OsIRE1 and OsbZIP50*, a well-known branch of UPR, and the expression of *OsbZIP50* (*At*bZIP60 ortholog), the second branch of UPR (Fig. 10). It was much higher in roots than shoots, once it was in direct contact with salt, and TM was reported to improve root growth hair (Lima et al., 2022), and upregulation of UPR genes promotes root elongation (Kim et al., 2018). Additionally, these results are in agreement with the literature, since UPR and endoplasmic reticulum-associated quality control were related to improved plant salt tolerance by seed priming and a possible mechanism of memory in plants (Tian et al., 2019).

Salt stress leads to impairment in water balance and the quick absorption of Na^+ ions causes negative plant-water relations (Balasubramaniam et al., 2023). TM-pretreatment increased this ratio in both shoots and roots in the presence of NaCl, which means it might have increased K^+ absorption and reduced Na^+ uptake (Fig. 6). It has been suggested that plant survival under salt stress requires a high cytosolic K^+/Na^+ ratio in the cytoplasm (Almeida et al., 2017), as well as the restriction of Na^+ accumulation in shoots under salt stress has been correlated with salt tolerance in rice (Almeida et al., 2017; Lutts et al., 1996). Although chloride is considered an essential micronutrient for plants, being involved in photosynthesis and stomatal regulation (Franco-Navarro et al., 2016; Shelke et al., 2019), in high concentrations it can lead to toxicity, bringing about several harms to the cell, such as increased ROS production, chlorophyll degradation, and reduction of chlorophyll synthesis and actual quantum yield of PSII electron transport (Shelke et al., 2019; Tavakkoli et al., 2012). Thus, the less Cl^- available/free, the better. TM-pre-treatment might have induced Cl^- compartmentation in root vacuoles, or probably contributed to Cl^- exclusion from mesophyll cells (Shelke et al., 2019). These results are in accordance with the exogenous application of nitric oxide (NO) in rice plants under salt stress, where the authors found that NO priming decreased both root and shoot Cl^- and Na^+ contents, therefore increasing water potential (Habib and Ashraf, 2014). It was corroborated by confocal microscopy, which showed that T025S150 seedlings exhibited lower cytosolic intensities of fluorescence probe in both roots and shoots, suggesting that TM-priming helped reduce the content of this ion, which is in agreement to previous results that indicate an relation among intensity of fluorescence and sodium uptake in rice (Gadelha et al., 2021). Additionally, proteins SOS act in the mechanism of sodium exclusion, particularly in roots (Ali et al., 2023). Here, the expression of *OsSOS1* was increased in both salt treatments, which may contribute to minimizing the accumulation of sodium in roots (Supplementary Table S5), corroborating the results described above.

4.3. ER induction improves antioxidant system and osmoprotectants

To cope with that extra toxicity, an efficient antioxidant system is necessary to be present or activated (Figs. 8 and 9), and non-enzymatic low molecular weight compounds such as beta-alanine and maltose (Figs. 10C and 11C). SOD can turn $\cdot O_2^-$, an extremely reactive ROS, into a less reactive one, H_2O_2, which will be used as substrate by CAT and GPOD, breaking it down into the non-toxic molecules H_2O and O_2 (Xu et al., 2010). Not only did these enzymes have their activities increased in both shoots and roots, induced by TM, but also the ROS levels, electrolyte leakage and the lipid peroxidation decreased, which match well with the elevated growth parameters, in relation to T0S150 seedlings, revealing that TM induces an antioxidant enzyme system that efficiently scavenges ROS, alleviating the deleterious effects of salt stress and therefore, leading to higher biomass and length. Indeed, the induction of ER response reduced the negative effects of salinity, decreasing ROS by enzyme activities (de Queiroz et al., 2020). The relation between ROS and ER response has been reported, in which ER stress activates the antioxidant system to reduce ROS, and ROS activates ER response in a dynamic duo (Ozgur et al., 2018).

Our results are also in accordance with other works, who tested 3 different priming agents (KNO_3, SiO_2 and SA) in rice seeds under drought conditions: mild (75 % field capacity), moderate (50 % FC) and severe, 25 % FC, and verified an increase in SOD, CAT and APX activities under all those conditions (Ali et al., 2021). Slightly different results were found using SiO_2 priming in rice seeds under 100 mM NaCl: aside from CAT, GPOD, APX and SOD had their activities increased in the presence of NaCl, which lead to a lower lipid peroxidation (Ali et al., 2021). This was due to an efficient antioxidant enzyme system, which helped reduce ROS levels and led to increased chlorophyll content. Such results can be corroborated by maize H_2O_2 leaf sprayed in the presence of NaCl, that increase in photosynthetic rate and in chlorophyll content in the primed plants (Gondim et al., 2013).

Furthermore, TM seed priming can prepare seedlings for severe conditions, such as high salinity, by activating an efficient antioxidant system coupled to an increase in osmoprotectants (Figs. 11 and 12, and Supplementary tables S6 and S7). For instance O-acetylserine, the direct precursor of cysteine, which generates, besides proteins, biotin, ethylene, polyamine, and GSH, which can directly or indirectly regulate the salinity stress response (Van Nguyen et al., 2021), beta-alanine (Parthasarathy et al., 2019), and maltose, which not only works as an osmoprotectant but provides cellular energy (Ibrahim and Abdellatif, 2016), which could help to explain higher germination percentages, germination speed index and lower mean germination time, as well as lengths and dry masses. Such results are corroborated by the exogenous

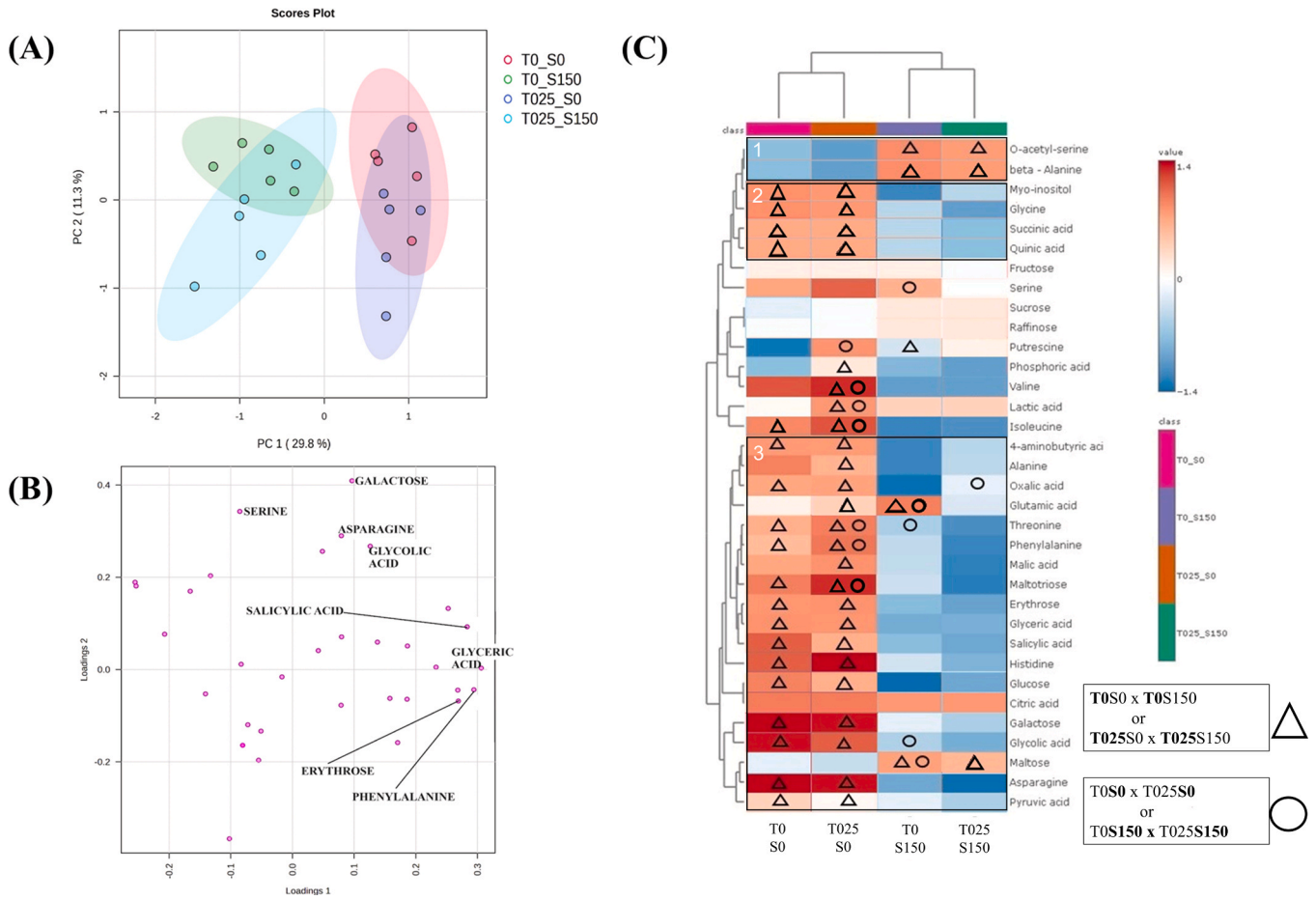

Fig. 11. Multivariate analysis of metabolites found in shoots. Principal components (PC) score plot (10 A), PCA loading plot (10B) and heatmap (10 C) of shoots of rice seedlings TM-primed and non-primed, grown in presence or absence of salinity. In the heatmap, triangle means statistical significance between treatments within the same TM concentration, whereas circle means significance between treatments with the same NaCl concentration based on Tukey test ($p \leq 0.05$) available on supplementary Table S7. The data represent the set of 5 biological repetitions.

application of nitric oxide in rice seeds under 150 mM (Tahjib-Ul-Arif et al., 2022), and primed rice seeds with H_2O_2 and submitted seedlings with 100 and 150 mM NaCl (Hemalatha et al., 2017). TM-pre-treaded seedlings displayed lower electrolyte leakage in shoots, but also showed higher osmotic potential in relation to non-TM-pretreated under salinity. Other possible explanation for that is TM-pre-treatment might have increased the productions of osmoprotectants, such as beta-alanine and maltose (Fig. 12C), as well as in roots the positive modulation of 4-aminobutyric acid, also known as GABA, an important molecule in plant defense to salt stress (Guo et al., 2023), besides the increased activities of antioxidant enzymes (Fig. 9).

4.4. TM seed priming modulates metabolites that may contribute to salt acclimation

Interesting, salinity significantly decreased the contents of organic acids in both shoots and roots. Nevertheless, TM-priming, under saline conditions, not only modulated amino acids and sugars, such as O-acetyserine, 4-aminobutyric acid, and maltose, but also increased these contents in relation to unprimed seedlings (Figs. 11C and 12C).

For shoots metabolites, O-acetylserine, beta-alanine, and maltose were considered key metabolites for salt response, independently of TM seed priming (Fig. 13). O-acetylserine is involved in not only cysteine biosynthesis, but also ethylene, polyamines, and glutathione, important molecules involved in salt tolerance (Van Nguyen et al., 2021). Beta-alanine, an important osmoprotectant and involved in coenzyme A biosynthesis, is crucial for the tricarboxylic acid cycle and fatty acid metabolism (Parthasarathy et al., 2019). These results might have contributed to higher photosynthetic pigment contents and higher plant growth (Fig. 3). Similar results reported that salt-tolerant rice genotypes exhibited positive modulation of beta-alanine and maltose under 150 mM NaCl (Gupta and De, 2017). Also, previous work reported that osmolyte accumulation (such as beta-alanine and proline) crosstalking with phytohormones (e.g. ethylene and ABA) led to NaCl resilience (Singh et al., 2022).

Concerning root metabolites, glutamic acid, raffinose, and O-acetylserine were considered key metabolites in TM-induced plants, which may help to alleviate NaCl toxicity (Fig. 13). Moreover, TM increased the modulation of other salt-responsive metabolites in roots, such as amino acids and other sugars, besides increasing metabolites whose contents had been reduced by salinity (Fig. 12C). Glutamic acid, or its anionic form, glutamate (Glu), is a unique primary metabolite in plants: in addition to its role as an amino acid for protein synthesis, Glu is a central metabolic hub connecting carbon (C), and nitrogen (N) metabolism, also serving as an N-donor for the biosynthesis of amino acids and other N-containing compounds. Most organic N compounds synthesized in the cell either directly or indirectly receive their N from Glu (Liao et al., 2022). On top of amino acid and N metabolism, Glu is a building block for essential biomolecules such as glutathione (GSH) and the cofactor folate (Liao et al., 2022). So, glutamate might have acted as carbon-donor to the TCA cycle, as some intermediates were down-modulated by salinity. Raffinose is a trisaccharide comprised by galactose, glucose and fructose that is ubiquitous in plants and has been demonstrated to play important roles in seed desiccation tolerance/seed

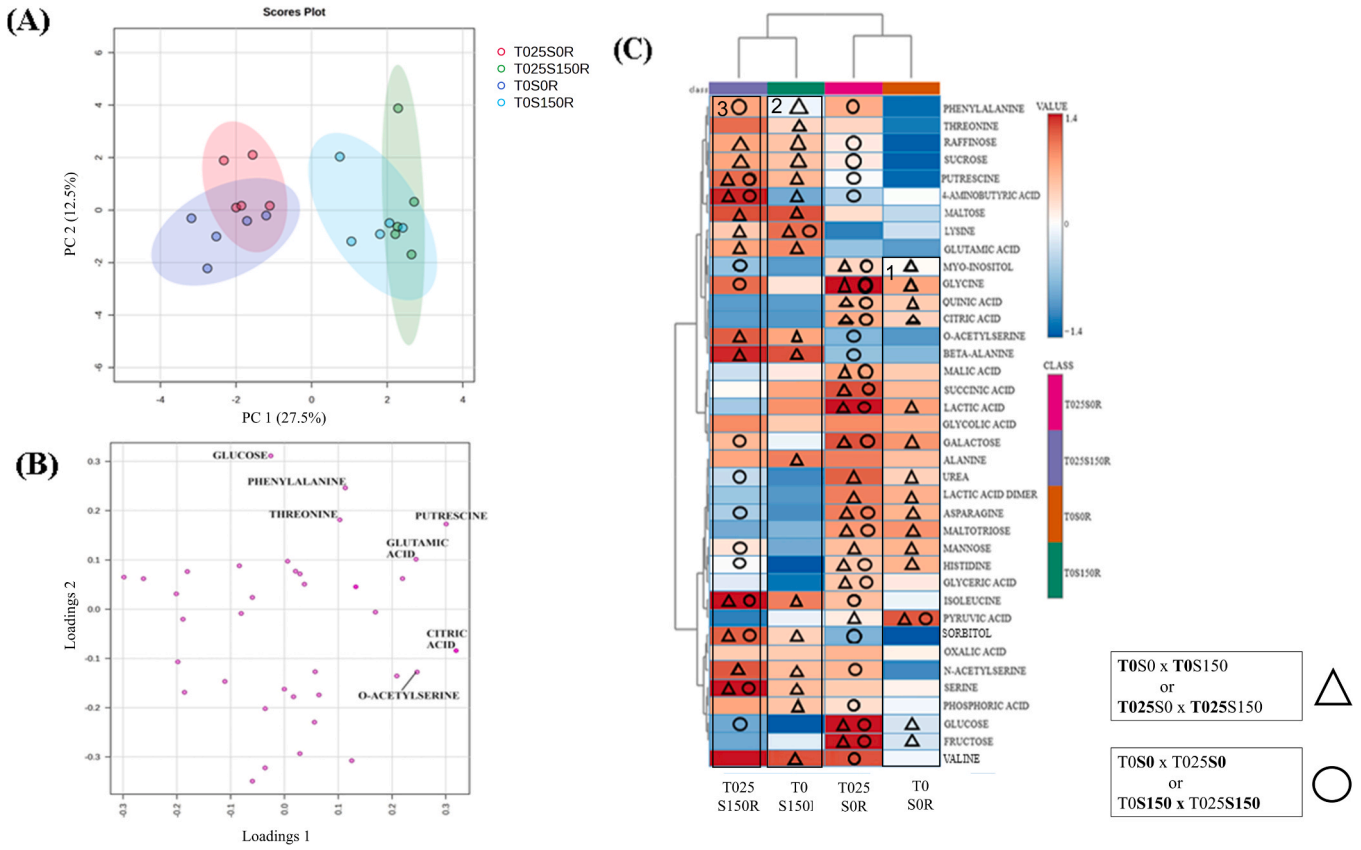

Fig. 12. Multivariate analysis of metabolites found in roots. Principal components (PC) score plot (A), PCA loading plot (B) and heatmap (C) of roots of rice seedling TM-primed or not and submitted or not to salinity. In the heatmap, triangle means statistical significance between treatments within the same TM concentration, whereas circle means significance between treatments with the same NaCl concentration based on Tukey test ($p \leq 0.05$) available on supplementary Table S8. The data represent the set of 5 biological repetitions.

storability; its synthesis is catalyzed by the enzymes galactol-synthase, which adds myo-inositol to UDP-galactose, thus generating galactinol, and raffinose-synthase, which incorporates galactose units from galactinol to sucrose, producing raffinose (Sengupta et al., 2015). Under salt/osmotic stress, genes related to its biosynthesis, such as *AtGolS* and *AtRS* are overexpressed, which highlights the importance of this sugar to cope with NaCl (Yan et al., 2022). Here, salinity decreased galactose and myo-inositol contents, but TM significantly increased them, which might have contributed to higher raffinose contents, and therefore, more energy to deal with Na toxicity. According, the metabolic flux of rice under salt stress revelead a positive modulation of this metabolite, evidencing its role in salt tolerance (Wanichthanarak et al., 2020).

On the other hand, putrescine, sorbitol, and asparagine were key metabolites in salt stress in the absence of TM. It has been reported that, in salt stress, sorbitol is usually accumulated, working as an osmoprotectant, playing a role in the osmotic adjustment (Pleyerová et al., 2022). In this study, it might have replenished either glucose or fructose pools to keep glycolysis functional, besides acting as an osmoprotectant, which might contribute to a higher osmotic potential, and provided energy (ATP), therefore alleviating Na^+ toxicity, which may be related to much higher ER gene expression. Putrescine (Put) is also a salt-responsive metabolite, which might led to NaCl acclimation, Put alleviated stress not only by inducing thylakoid membrane lipid peroxidation by increasing unsaturated fatty acid content but also by upregulating ATPase, thus facilitating the Na^+ efflux (Ghalati et al., 2020). These results are in accordance with literature (Rajkumari et al., 2023), who also noticed that the concentration of these amino acids and putrescine increased in salt-tolerant rice genotypes, which matches with TM-primed metabolites.

It is also worth pointing out that, although TM-priming appears to be an approach for salt acclimation in plants, inducing the benefits of ER response, it does present some considerations. TM should be used in small amounts, as it inhibits protein N-glycosylation in eukaryotes and can cell death at high concentrations (Price and Link, 2024). However, our results did not show relevant toxicity between TM-treated and control seeds. One alternative is to find some much lower toxic TM analogs by chemically reducing the N-acyl double bond or both the N-acyl and uridyl double bonds (Price et al., 2019). Likewise, our work highlights the efficiency of endoplasmic reticulum induction against salinity. It may improve ER control quality, osmotic and ionic adjustments, and antioxidant effects to maintain primary metabolism and consequently the growth. This approach may guide the selection of candidate genes for plant breeding and transgenic lines against single or multiple abiotic stresses, such as salinity, heat, and drought, as well as biotic stresses.

5. Conclusion

Overall, TM priming alleviated the deleterious effects of salt stress in 10 DAT rice seedlings which induced higher biomasses and physiological parameters but also might have helped pump Na^+ out of the cell. It activates unfolded protein response by the expression of *OsIRE1 and OsbZIP50* that may contribute to an efficient antioxidant system and the positive modulation of primary metabolites (e.g maltose, glutamic acid, O-acetylserine and lysine) involved in energy synthesis or production of intermediates of TCA cycle (such as malic acid and succinic acid). Besides, the unprecedented TM priming reveals to be a promising approach for salt stress acclimation. However, more studies are necessary for a better comprehension of the theme and its relation to ER response, identifying genes and proteins that activated by priming, as well as other

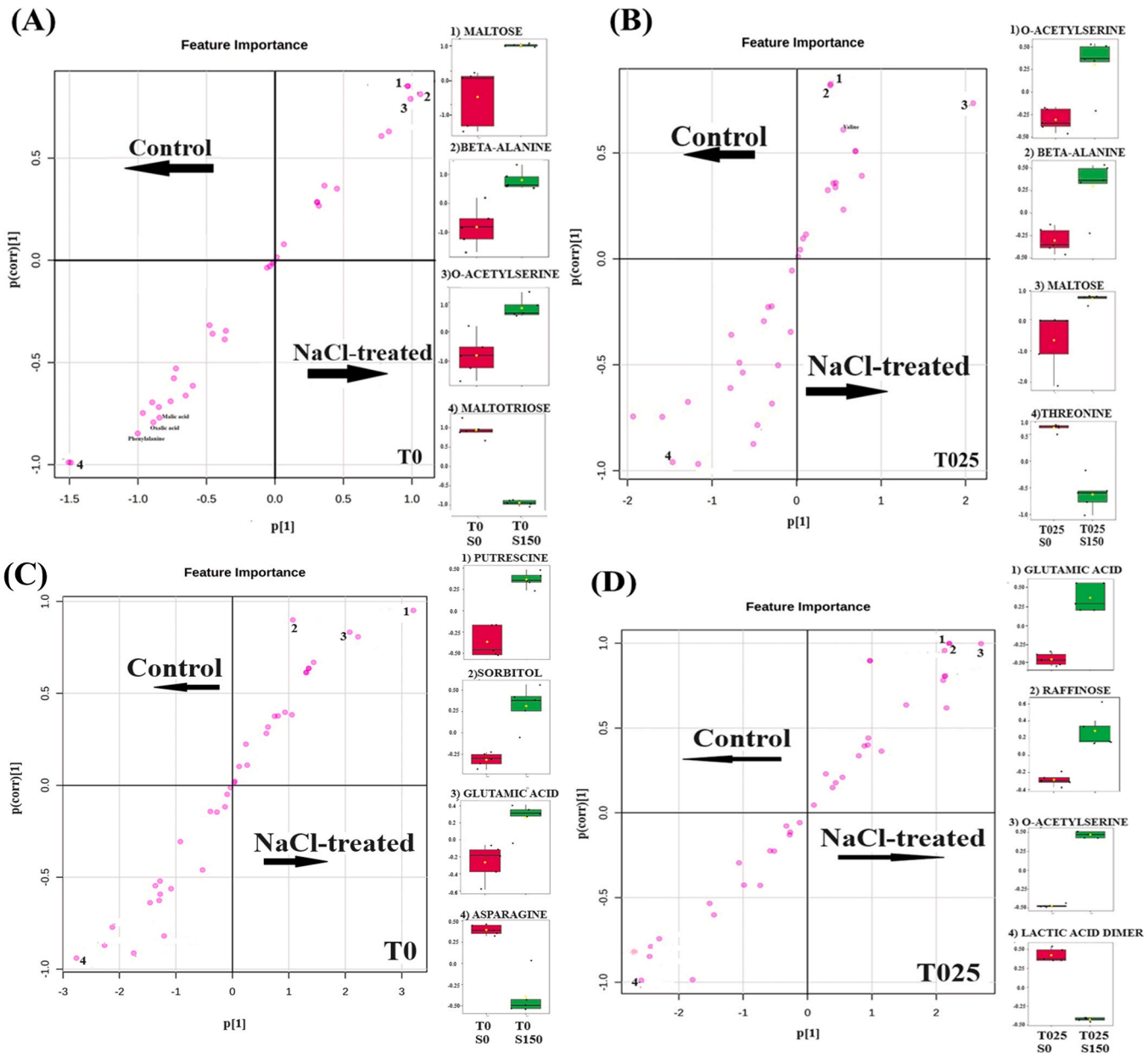

Fig. 13. S-plots from orthogonal projections to latent structures discriminant analysis (OPLS-DA) shoots of rice seedlings with TM at 0 μg. mL^{-1} (A) at 0 mM NaCl (Control) or 150 mM NaCl (NaCl-treated), shoots with TM at 0.25 μg. mL^{-1} (B) at 0 mM NaCl (Control) or 150 mM NaCl (NaCl-treated), and roots with TM at 0 μg. mL^{-1} (C) at 0 mM NaCl (Control) or 150 mM NaCl (NaCl-treated), and TM at 0.25 μg. mL^{-1} (D) at 0 mM NaCl (Control) or 150 mM NaCl (NaCl-treated). The three most significant metabolites that had the major contribution to NaCl-treated (upper right corner) and Control seedlings (lower left corner) were highlighted, and their relative content were provided on the right of each plot of shoot rice seedlings. The data represent the set of 5 biological repetitions.

priming agents or analogs to cause less effect in plant system.

CRediT authorship contribution statement

Isabelle Mary Costa Pereira: Writing – review & editing, Methodology, Formal analysis, Data curation. **Igor Rafael Sousa Costa:** Writing – review & editing, Methodology, Formal analysis, Data curation. **Francisco Lucas Pacheco Cavalcante:** Writing – review & editing, Methodology, Formal analysis, Data curation. **Ítalo Antônio Cotta Coutinho:** Writing – review & editing, Supervision, Methodology, Data curation. **Murilo Siqueira Alves:** Writing – review & editing, Supervision, Methodology, Data curation. **Stelamaris de Oliveira Paula-Marinho:** Writing – review & editing, Writing – original draft, Methodology, Data curation. **Eneas Gomes-Filho:** Writing – review & editing, Writing – original draft, Supervision, Conceptualization. **Humberto Henrique de Carvalho:** Writing – review & editing, Writing – original draft, Supervision, Resources, Project administration, Methodology, Investigation, Data curation, Conceptualization. **Francisco Dalton Barreto de Oliveira:** Writing – review & editing, Writing – original draft, Methodology, Formal analysis, Data curation, Conceptualization.

Funding

This work was supported by Conselho Nacional de Desenvolvimento Científico e Tecnológico (CNPq), process 408118/2021–0.

Declaration of Competing Interest

The authors declare that they have no known competing financial interests or personal relationships that could have appeared to influence

the work reported in this paper.

Acknowledgments

We would like to thank to Cryogenics Center's Physics Department of Federal University of Ceará for nitrogen suppling. Thanks to Coordenação de Aperfeiçoamento de Pessoal de Nível Superior (CAPES), Fundação Cearense de Apoio ao Desenvolvimento Científico e Tecnológico (FUNCAP), and Conselho Nacional de desenvolvimento Científico e Tecnológico (CNPq) for student's scholarship and HHC Productivity Scholarship 306117/2022–3.

Appendix A. Supporting information

Supplementary data associated with this article can be found in the online version at doi:10.1016/j.plantsci.2025.112567.

Data availability

No data was used for the research described in the article.

References

L.G. Ali, R. Nulit, M.H. Ibrahim, C.Y.S. Yien, Efficacy of KNO_3, SiO_2 and SA priming for improving emergence, seedling growth and antioxidant enzymes of rice (*Oryza sativa*), under drought, Sci. Rep. 11 (2021) 3864, https://doi.org/10.1038/s41598-021-83434-3.

A. Ali, V. Petrov, D.J. Yun, T. Gechev, Revisiting plant salt tolerance: novel components of the SOS pathway, Trends Plant Sci. 28 (2023) 1060–1069, https://doi.org/10.1016/j.tplants.2023.04.003.

D.M. Almeida, M.M. Oliveira, N.J.M. Saibo, Regulation of Na^+ and K^+ homeostasis in plants: towards improved salt stress tolerance in crop plants, Genet. Mol. Biol. 40 (2017) 326–345, https://doi.org/10.1590/1678-4685-gmb-2016-0106.

E.K. Astani, S. Malek Zadeh, N.S. Hsu, K.H. Lin, S. Sardari, T.L. Li, Intermolecular interactions of nucleoside antibiotic tunicamycin with on-target MraYCB-TUN and off-target DPAGT1-TUN in the active sites delineated by quantum mechanics/molecular mechanics calculations, ACS Omega 7 (2022) 32970–32987, https://doi.org/10.1021/acsomega.2c02213.

K.P.R. Aswathi, H.M. Kalaji, J.T. Puthur, Seed priming of plants aiding in drought stress tolerance and faster recovery: a review, Plant Growth Regul. 97 (2022) 235–253, https://doi.org/10.1007/s10725-021-00755-z.

A. Ayaz, C. Hu, Y. Li, Current advances and future prospects of ER stress signaling and its chemical mitigation in plants, Plant Growth Regul. 104 (2024) 89–93, https://doi.org/10.1007/s10725-024-01172-8.

T. Balasubramaniam, G. Shen, N. Esmaeili, H. Zhang, Plants' response mechanisms to salinity stress, Plants 12 (2023) 1–22, https://doi.org/10.3390/plants12122253.

Y. Bao, D.C. Bassham, S.H. Howell, A functional unfolded protein response is required for normal vegetative development, Plant Physiol. 179 (2019) 1834–1843, https://doi.org/10.1104/pp.18.01261.

E. Bassil, S. Zhang, H. Gong, H. Tajima, E. Blumwald, Cation specificity of vacuolar NHX-type cation/H^+ Antiporters 1[OPEN, Plant Physiol. 179 (2019) 616–629, https://doi.org/10.1104/pp.18.01103.

I. Beaugelin, A. Chevalier, S. D'Alessandro, B. Ksas, M. Havaux, Endoplasmic reticulum-mediated unfolded protein response is an integral part of singlet oxygen signalling in plants, Plant J. 102 (2020) 1266–1280, https://doi.org/10.1111/tpj.14700.

R.F. Beers, I.W. Sizer, A spectrophotometric method for measuring the breakdown of hydrogen peroxide by catalase, J. Biol. Chem. 195 (1952) 133–140. ⟨http://www.ncbi.nlm.nih.gov/pubmed/14938361⟩.

N. Ben Amor, A. Jiménez, M. Boudabbous, F. Sevilla, C. Abdelly, Chloroplast Implication in the Tolerance to Salinity of the Halophyte Cakile maritima, Russ. J. Plant Physiol. 67 (2020) 507–514, https://doi.org/10.1134/S1021443720030048.

W.F. Beyer, I. Fridovich, Assaying for superoxide dismutase activity: some large consequences of minor changes in conditions, Anal. Biochem 161 (1987) 559–566, https://doi.org/10.1016/0003-2697(87)90489-1.

M.M. Bradford, A rapid and sensitive method for the quantification of microgram quantities od protein utilizing the principle of protein-dye binding, Anal. Biochem 72 (1976) 246–254.

E. Brenya, E. Dutta, B. Herron, L.H. Walden, D.M. Roberts, B.M. Binder, Ethylene-mediated metabolic priming increases photosynthesis and metabolism to enhance plant growth and stress tolerance, PNAS Nexus 2 (2023), https://doi.org/10.1093/pnasnexus/pgad216.

B. Çakır Aydemir, C. Yüksel Özmen, U. Kibar, F. Mutaf, P.B. Büyük, M. Bakır, A. Ergül, Salt stress induces endoplasmic reticulum stress-responsive genes in a grapevine rootstock, PLoS One 15 (2020) e0236424, https://doi.org/10.1371/journal.pone.0236424.

A.N. Callister, S.K. Arndt, M.A. Adams, Comparison of four methods for measuring osmotic potential of tree leaves, Physiol. Plant 127 (2006) 383–392, https://doi.org/10.1111/j.1399-3054.2006.00652.x.

F.L.P. Cavalcante, S.J. da Silva, L.S. Lopes, S.O. Paula-Marinho, M.I.F. Guedes, E. Gomes-Filho, H.H. de Carvalho, Unveiling a differential metabolite modulation of sorghum varieties under increasing tunicamycin-induced endoplasmic reticulum stress, Cell Stress Chaperon-.-. (2023), https://doi.org/10.1007/s12192-023-01382-5.

J.M. Cheeseman, Hydrogen peroxide concentrations in leaves under natural conditions, J. Exp. Bot. 57 (2006) 2435–2444, https://doi.org/10.1093/jxb/erl004.

K.H. Chele, M.M. Tinte, L.A. Piater, I.A. Dubery, F. Tugizimana, Soil salinity, a serious environmental issue and plant responses: a metabolomics perspective, Metabolites 11 (2021), https://doi.org/10.3390/metabo11110724.

Y. Cho, Arabidopsis AGB1 participates in salinity response through bZIP17-mediated unfolded protein response, BMC Plant Biol. 24 (2024) 586, https://doi.org/10.1186/s12870-024-05296-x.

L. Colin, F. Ruhnow, J.K. Zhu, C. Zhao, Y. Zhao, S. Persson, The cell biology of primary cell walls during salt stress, Plant Cell 35 (2023) 201–217, https://doi.org/10.1093/plcell/koac292.

I.R.S. Costa, F.L.P. Cavalcante, F.R. Cavalcanti, C. de Freitas Fernandes, E. Gomes-Filho, K.M. Canuto, H.H. de Carvalho, Metabolomic exhibits different profiles and potential biomarkers of *Vitis* spp. co-cultivated with *Fusarium oxysporum* for short, medium, and long times, Physiol. Plant 175 (2023) e13918, https://doi.org/10.1111/ppl.13918.

C.S. de Queiroz, I.M.C. Pereira, K.R.P. Lima, R.S.C. Bret, M.S. Alves, E. Gomes-Filho, H. H. de Carvalho, Combined NaCl and DTT diminish harmful ER-stress effects in the sorghum seedlings CSF 20 variety, Plant Physiol. Biochem 147 (2020) 223–234, https://doi.org/10.1016/j.plaphy.2019.12.013.

M.L. Dionisio-Sese, S. Tobita, Antioxidant responses of rice seedlings to salinity stress, Plant Sci. 135 (1998) 1–9, https://doi.org/10.1016/S0168-9452(98)00025-9.

E. Malavolta G.C. VItti S.A. de Oliveira Avaliação do estado nutricional das plantas; princípios e aplicações 1989 Piracicaba.

E.F. Elstner, A. Heupel, Inhibition of nitrite formation from hydroxylammoniumchloride: a simple assay for superoxide dismutase, Anal. Biochem 70 (1976) 616–620, https://doi.org/10.1016/0003-2697(76)90488-7.

D.F. Ferreira, Sisvar: a computer statistical analysis system, Ciência e Agrotecnologia 35 (2011) 1039–1042, https://doi.org/10.1590/S1413-70542011000600001.

J.D. Franco-Navarro, J. Brumós, M.A. Rosales, P. Cubero-Font, M. Talón, J. M. Colmenero-Flores, Chloride regulates leaf cell size and water relations in tobacco plants, J. Exp. Bot. 67 (2016) 873–891, https://doi.org/10.1093/jxb/erv502.

C.G. Gadelha, I.A.C. Coutinho, S.K.P. Pinheiro, E.C. Miguel, H.H. Carvalho, L.S. Lopes, E. Gomes-Filho, Sodium uptake and transport regulation, and photosynthetic efficiency maintenance as the basis of differential salt tolerance in rice cultivars, Environ. Exp. Bot. 192 (2021) 104654, https://doi.org/10.1016/j.envexpbot.2021.104654.

S.A. Ganie, N. McMulkin, A. Devoto, The role of priming and memory in rice environmental stress adaptation: current knowledge and perspectives, Plant Cell Environ. 47 (2024) 1895–1915, https://doi.org/10.1111/PCE.14855.

M. Georgieva, V. Vassileva, Stress management in plants: examining provisional and unique dose-dependent responses, Int. J. Mol. Sci. 24 (2023) 5105, https://doi.org/10.3390/ijms24065105.

R.E. Ghalati, M. Shamili, A. Homaei, Effect of putrescine on biochemical and physiological characteristics of guava (*Psidium guajava* L.) seedlings under salt stress, Sci. Hortic. (Amst.). 261 (2020) 108961, https://doi.org/10.1016/j.scienta.2019.108961.

F.A. Gondim, R.D.S. Miranda, E. Gomes-Filho, J.T. Prisco, Enhanced salt tolerance in maize plants induced by H_2O_2 leaf spraying is associated with improved gas exchange rather than with non-enzymatic antioxidant system, Theor. Exp. Plant Physiol. 25 (2013) 251–260, https://doi.org/10.1590/S2197-00252013000400003.

K. Guo, T. Glatter, N. Paczia, W. Liesack, Asparagine uptake: a cellular strategy of methylocystis to combat severe salt stress, Appl. Environ. Microbiol 89 (2023), https://doi.org/10.1128/aem.00113-23.

P. Gupta, B. De, Metabolomics analysis of rice responses to salinity stress revealed elevation of serotonin, and gentisic acid levels in leaves of tolerant varieties, Plant Signal. Behav. 12 (2017) e1335845, https://doi.org/10.1080/15592324.2017.1335845.

N. Habib, M. Ashraf, Effect of exogenously applied nitric oxide on water relations and ionic composition of rice (*Oryza sativa* L.) plants under salt stress, Pak. J. Bot. 46 (2014) 111–116.

M. Hasanuzzaman, M.H.M.B. Bhuyan, K. Parvin, T.F. Bhuiyan, T.I. Anee, K. Nahar, M. S. Hossen, F. Zulfiqar, M.M. Alam, M. Fujita, Regulation of ROS metabolism in plants under environmental stress: a review of recent experimental evidence, Int. J. Mol. Sci. 21 (2020) 1–44, https://doi.org/10.3390/ijms21228695.

S. Hayashi, Y. Wakasa, F. Takaiwa, Recent advances in understanding the control of secretory proteins by the unfolded protein response in plants, Int. J. Mol. Sci. 14 (2013) 9396–9407, https://doi.org/10.3390/ijms14059396.

S. Hayashi, Y. Wakasa, H. Takahashi, T. Kawakatsu, F. Takaiwa, Signal transduction by IRE1-mediated splicing of bZIP50 and other stress sensors in the endoplasmic reticulum stress response of rice, Plant J. 69 (2012) 946–956, https://doi.org/10.1111/j.1365-313X.2011.04844.x.

R.L. Heath, L. Packer, Photoperoxidation in isolated chloroplasts, Arch. Biochem. Biophys. (1968), https://doi.org/10.1016/0003-9861(68)90654-1.

G. Hemalatha, J. Renugadevi, T. Eevera, Studies on seed priming with hydrogen peroxide for mitigating salt stress in rice, Int. J. Curr. Microbiol. Appl. Sci. 6 (2017) 691–695, https://doi.org/10.20546/ijcmas.2017.606.081.

A. Hidayah, R.R. Nisak, F.A. Susanto, T.R. Nuringtyas, N. Yamaguchi, Y.A. Purwestri, Seed halopriming improves salinity tolerance of some rice cultivars during seedling stage, Bot. Stud. 63 (2022) 24, https://doi.org/10.1186/s40529-022-00354-9.

S.H. Howell, When is the unfolded protein response not the unfolded protein response? Plant Sci. 260 (2017) 139–143, https://doi.org/10.1016/j.plantsci.2017.03.014.

S.H. Howell, Evolution of the unfolded protein response in plants, Plant. Cell Environ. 44 (2021) 2625–2635, https://doi.org/10.1111/pce.14063.
H.A. Ibrahim, Y.M.R. Abdellatif, Effect of maltose and trehalose on growth, yield and some biochemical components of wheat plant under water stress, Ann. Agric. Sci. 61 (2016) 267–274, https://doi.org/10.1016/j.aoas.2016.05.002.
I. Iwasaki, S. Utsumi, T. Ozawa, New colorimetric determination of chloride using mercuric thiocyanate and ferric ion, Bull. Chem. Soc. Jpn. 25 (1952), 226–226.
S. Je, Y. Lee, Y. Yamaoka, Effect of common ER stress-inducing drugs on the growth and lipid phenotypes of chlamydomonas and arabidopsis, Plant Cell Physiol. 64 (2023) 392–404, https://doi.org/10.1093/pcp/pcac154.
Q.S. Jiao, G.T. Niu, F.F. Wang, J.Y. Dong, T.S. Chen, C.F. Zhou, Z. Hong, N-glycosylation regulates photosynthetic efficiency of Arabidopsis thaliana, Photosynthetica 58 (2020) 72–79, https://doi.org/10.32615/ps.2019.153.
M.O. Khan, M. Irfan, A. Muhammad, I. Ullah, S. Nawaz, M.K. Khalil, M. Ahmad, A practical and economical strategy to mitigate salinity stress through seed priming, Front. Environ. Sci. 10 (2022b) 1–14, https://doi.org/10.3389/fenvs.2022.991977.
I. Khan, A. Muhammad, M.U. Chattha, M. Skalicky, M. Bilal Chattha, M. Ahsin Ayub, M. Rizwan Anwar, W. Soufan, M.U. Hassan, M.A. Rahman, M. Brestic, M. Zivcak, A. El Sabagh, Mitigation of salinity-induced oxidative damage, growth, and yield reduction in fine rice by sugarcane press mud application, Front. Plant Sci. 13 (2022a), https://doi.org/10.3389/fpls.2022.840900.
J.S. Kim, K. Mochida, K. Shinozaki, ER stress and the unfolded protein response: homeostatic regulation coordinate plant survival and growth, Plants 11 (2022), https://doi.org/10.3390/plants11233197.
J.-S. Kim, K. Yamaguchi-Shinozaki, K. Shinozaki, ER-anchored transcription factors bZIP17 and bZIP28 regulate root elongation, Plant Physiol. (2018), https://doi.org/10.1104/pp.17.01414.
A. Kumari, M.S. Bhinda, S. Sharma, M.K. Chitara, A. Debnath, C. Maharana, M. Parihar, B. Sharma. ROS Regulation Mechanism for Mitigation of Abiotic Stress in Plants, 2022, https://doi.org/10.5772/intechopen.99845.
L.G. Labouriau A germinação das sementes 1983.
M. Laxa, M. Liebthal, W. Telman, K. Chibani, K.J. Dietz, The role of the plant antioxidant system in drought tolerance, Antioxidants 8 (2019), https://doi.org/10.3390/antiox8040094.
N. Li, Z. Huang, L. Ding, H. Shi, M. Hong, Endoplasmic reticulum unfolded protein response modulates the adaptation of *Trachemys scripta elegans* in salinity water, Comp. Biochem. Physiol. Part C. Toxicol. Pharm. 248 (2021) 109102, https://doi.org/10.1016/j.cbpc.2021.109102.
H.-S. Liao, Y.-H. Chung, M.-H. Hsieh, Glutamate: a multifunctional amino acid in plants, Plant Sci. 318 (2022) 111238, https://doi.org/10.1016/j.plantsci.2022.111238.
K.R.P. Lima, F.L.P. Cavalcante, S. de, O. Paula-Marinho, I.M.C. Pereira, L. de, S. Lopes, J. V.S. Nunes, Í.A.C. Coutinho, E. Gomes-Filho, H.H. De Carvalho, Metabolomic profiles exhibit the influence of endoplasmic reticulum stress on sorghum seedling growth over time, Plant Physiol. Biochem 170 (2022) 192–205, https://doi.org/10.1016/j.plaphy.2021.11.041.
J. Lisec, N. Schauer, J. Kopka, L. Willmitzer, A.R. Fernie, Gas chromatography mass spectrometry–based metabolite profiling in plants, Nat. Protoc. 1 (2006) 387–396, https://doi.org/10.1038/nprot.2006.59.
Y. Liu, Y. Lv, A. Wei, M. Guo, Y. Li, J. Wang, X. Wang, Y. Bao, Unfolded protein response in balancing plant growth and stress tolerance, Front. Plant Sci. 13 (2022a), https://doi.org/10.3389/fpls.2022.1019414.
Z. Liu, C. Ma, L. Hou, X. Wu, D. Wang, L. Zhang, P. Liu, Exogenous SA affects rice seed germination under salt stress by regulating Na+ /K+ balance and endogenous GAs and ABA homeostasis, Int. J. Mol. Sci. 23 (2022b), https://doi.org/10.3390/ijms23063293.
Y. Liu, S. Tian, T. Chen, Endoplasmic reticulum homeostasis in plant–pathogen interactions: new scenarios for an old story, J. Exp. Bot. 76 (2025) 277–284, https://doi.org/10.1093/jxb/erae404.
K.J. Livak, T.D. Schmittgen, Analysis of Relative Gene Expression Data Using Real-Time Quantitative PCR and the 2−ΔΔCT Method, Methods 25 (2001) 40–408, https://doi.org/10.1006/meth.2001.1262.
S.-J. Lu, Z.-T. Yang, L. Sun, L. Sun, Z.-T. Song, J.-X. Liu, Conservation of IRE1-regulated bZIP74 mRNA unconventional splicing in rice (*Oryza sativa* L.) involved in ER stress responses, Mol. Plant 5 (2012) 504–514, https://doi.org/10.1093/mp/ssr115.
S. Lutts, J.M. Kinet, J. Bouharmont, Effects of salt stress on growth, mineral nutrition and proline accumulation in relation to osmotic adjustment in rice (*Oryza sativa* L.) cultivars differing in salinity resistance, Kluwer Acad. Publ. (1996).
J.D. Maguire, Speed of germination—aid in selection and evaluation for seedling emergence and vigor 1, Crop Sci. 2 (1962) 176–177, https://doi.org/10.2135/cropsci1962.0011183x000200020033x.
H. Manghwar, J. Li, Endoplasmic reticulum stress and unfolded protein response signaling in plants, Int. J. Mol. Sci. 23 (2022) 828, https://doi.org/10.3390/ijms23020828.
M.M.F. Mansour, E.F. Ali, K.H.A. Salama, Does seed priming play a role in regulating reactive oxygen species under saline conditions?. React. Oxyg. Nitrogen Sulfur Species Plants Wiley, 2019, pp. 437–488, https://doi.org/10.1002/9781119468677.ch18.
A.A.E. Méndez, L.B. Pena, M.P. Benavides, S.M. Gallego, Priming with NO controls redox state and prevents cadmium-induced general up-regulation of methionine sulfoxide reductase gene family in Arabidopsis, Biochimie 131 (2016) 128–136, https://doi.org/10.1016/J.BIOCHI.2016.09.021.
K. Mishiba, Y. Iwata, T. Mochizuki, A. Matsumura, N. Nishioka, R. Hirata, N. Koizumi, Unfolded protein-independent IRE1 activation contributes to multifaceted developmental processes in Arabidopsis, Life Sci. Alliance 2 (2019) e201900459, https://doi.org/10.26508/lsa.201900459.
R. Mukhopadhyay, B. Sarkar, H.S. Jat, P.C. Sharma, N.S. Bolan, Soil salinity under climate change: challenges for sustainable agriculture and food security, J. Environ. Manag. 280 (2021), https://doi.org/10.1016/j.jenvman.2020.111736.
Y. Nagashima, K. Mishiba, E. Suzuki, Y. Shimada, Y. Iwata, N. Koizumi, Arabidopsis IRE1 catalyses unconventional splicing of bZIP60 mRNA to produce the active transcription factor, Sci. Rep. 1 (2011) 29, https://doi.org/10.1038/srep00029.
Y. Nakano, K. Asada, Hydrogen peroxide is scavenged by ascorbate-specific peroxidase in spinach chloroplasts, Plant Cell Physiol. 22 (1981) 867–880.
G.M. Nawkar, E.S. Lee, R.M. Shelake, J.H. Park, S.W. Ryu, C.H. Kang, S.Y. Lee, Activation of the transducers of unfolded protein response in plants, Front. Plant Sci. 9 (2018) 1–10, https://doi.org/10.3389/fpls.2018.00214.
M. Ohta, F. Takaiwa, OsERdj7 is an ER-resident J-protein involved in ER quality control in rice endosperm, J. Plant Physiol. 245 (2020) 153109, https://doi.org/10.1016/j.jplph.2019.153109.
R. Ozgur, B. Uzilday, Y. Iwata, N. Koizumi, I. Turkan, Interplay between the unfolded protein response and reactive oxygen species: a dynamic duo, J. Exp. Bot. 69 (2018) 3333–3345, https://doi.org/10.1093/jxb/ery040.
C.J. Park, J.M. Park, Endoplasmic reticulum plays a critical role in integrating signals generated by both biotic and abiotic stress in plants, Front. Plant Sci. 10 (2019a), https://doi.org/10.3389/fpls.2019.00399.
C.-J. Park, J.M. Park, Endoplasmic reticulum plays a critical role in integrating signals generated by both biotic and abiotic stress in plants, Front. Plant Sci. 10 (2019b) 1–8, https://doi.org/10.3389/fpls.2019.00399.
A. Parthasarathy, M.A. Savka, A.O. Hudson, The synthesis and role of β-alanine in plants, Front. Plant Sci. 10 (2019) 921, https://doi.org/10.3389/fpls.2019.00921.
I. Pleyerová, J. Hamet, H. Konrádová, H. Lipavská, Versatile roles of sorbitol in higher plants: luxury resource, effective defender or something else? Planta 256 (2022) 13, https://doi.org/10.1007/s00425-022-03925-z.
N.P.J. Price, M.A. Jackson, V. Singh, T.M. Hartman, J.A. Blackburn, P.F. Dowd, Synergistic enhancement of beta-lactam antibiotics by modified tunicamycin analogs TunR1 and TunR2, J. Antibiot. 72 (2019) 807–815, https://doi.org/10.1038/s41429-019-0220-x.
P.J. Price, B.A. Link, marinum -zebrafish TB infection model 77 (2024) 245–256, https://doi.org/10.1038/s41429-023-00694-z.The.
N. Rajkumari, S. Chowrasia, J. Nishad, S.A. Ganie, T.K. Mondal, Metabolomics-mediated elucidation of rice responses to salt stress, Planta 258 (2023), https://doi.org/10.1007/s00425-023-04258-1.
Rasband, W., ImageJ, U. S. Natl. Institutes Heal. Bethesda, Maryland, USA (2016).
S. Reyes-Impellizzeri, A.A. Moreno, The endoplasmic reticulum role in the plant response to abiotic stress, Front. Plant Sci. 12 (2021) 1–7, https://doi.org/10.3389/fpls.2021.755447.
P. Roder, C. Hille, ANG-2 for quantitative Na^+ determination in living cells by time-resolved fluorescence microscopy, Photochem. Photobiol. Sci. 13 (2014) 1699–1710, https://doi.org/10.1039/c4pp00061g.
T. Rossatto, G.M. Souza, M.N. do Amaral, P.A. Auler, M.M. Pérez-Alonso, S. Pollmann, E. J.B. Braga, Cross-stress memory: salt priming at vegetative growth stages improves tolerance to drought stress during grain-filling in rice plants, Environ. Exp. Bot. 206 (2023), https://doi.org/10.1016/j.envexpbot.2022.105187.
S. Sengupta, S. Mukherjee, P. Basak, A.L. Majumder, Significance of galactinol and raffinose family oligosaccharide synthesis in plants, Front. Plant Sci. 6 (2015) 1–11, https://doi.org/10.3389/fpls.2015.00656.
I. Sergiev, V. Alexieva, E. Karanov, Effect of spermine, atrazine and combination between them on some endogenous protective systems and stress markers in plants, Proc. Bulg. Acad. Sci. 51 (1997) 121–124.
D. Shelke, G. Nikalje, T. Nikam, P. Maheshwari, D. Punita, K. Rao, P. Kavi Kishor, P. Suprasanna, Chloride Cl^- uptake, transport, and regulation in plant salt tolerance. Mol. Plant Abiotic Stress, Wiley, 2019, pp. 241–268, https://doi.org/10.1002/9781119463665.ch13.
D. Singh, Juggling with reactive oxygen species and antioxidant defense system – a coping mechanism under salt stress, Plant Stress 5 (2022), https://doi.org/10.1016/j.stress.2022.100093.
P. Singh, K.K. Choudhary, N. Chaudhary, S. Gupta, M. Sahu, B. Tejaswini, S. Sarkar, Salt stress resilience in plants mediated through osmolyte accumulation and its crosstalk mechanism with phytohormones, Front. Plant Sci. 13 (2022), https://doi.org/10.3389/fpls.2022.1006617.
R. Strasser, G. Seifert, M.S. Doblin, K.L. Johnson, C. Ruprecht, F. Pfrengle, A. Bacic, J. M. Estevez, Cracking the "sugar code": a snapshot of N- and O-glycosylation pathways and functions in plants cells, Front. Plant Sci. 12 (2021), https://doi.org/10.3389/fpls.2021.640919.
M. Tahjib-Ul-Arif, X. Wei, I. Jahan, M. Hasanuzzaman, Z.H. Sabuj, F. Zulfiqar, J. Chen, R. Iqbal, K.M.G. Dastogeer, A.A.M. Sohag, S.H. Tonny, I. Hamid, I. Al-Ashkar, M. Mirzapour, A. El Sabagh, Y. Murata, Exogenous nitric oxide promotes salinity tolerance in plants: a meta-analysis, Front. Plant Sci. 13 (2022) 1–21, https://doi.org/10.3389/fpls.2022.957735.
H. Tang, H. Zhu, Specific changes in morphology and dynamics of plant mitochondria under abiotic stress, Horticulturae 9 (2023), https://doi.org/10.3390/horticulturae9010011.
E. Tavakkoli, F. Fatehi, P. Rengasamy, G.K. McDonald, A comparison of hydroponic and soil-based screening methods to identify salt tolerance in the field in barley, J. Exp. Bot. 63 (2012) 3853–3868, https://doi.org/10.1093/jxb/ers085.
P. Theerakulpisut, N. Kanawapee, B. Panwong, Seed priming alleviated salt stress effects on rice seedlings by improving Na^+ /K^+ and maintaining membrane integrity, Int. J. Plant Biol. 7 (2016) 53–58, https://doi.org/10.4081/pb.2016.6402.
L. Tian, Y. Zhang, E. Kang, H. Ma, H. Zhao, M. Yuan, L. Zhu, Y. Fu, Basic-leucine zipper 17 and Hmg-CoA reductase degradation 3A are involved in salt acclimation memory

in Arabidopsis, J. Integr. Plant Biol. 61 (2019) 1062–1084, https://doi.org/10.1111/jipb.12744.
H. Urbanek, E. Kuzniak-Gebarowska, H.L. (Poland)., Elicitation of defence responses in bean leaves by *Botrytis cinerea* polygalacturonase, Acta Physiol. Plant. 13 (1991).
T. Van Nguyen, J.-I. Kim, C.-R. Park, M.-S. Chung, C.S. Kim, Increased cysteine accumulation is essential for salt stress tolerance in arabidopsis halotolerance 2-like (AHL)-overexpressing transgenic plants, J. Plant Biol. 64 (2021) 475–485, https://doi.org/10.1007/s12374-021-09320-7.
K. Wanichthanarak, C. Boonchai, T. Kojonna, S. Chadchawan, W. Sangwongchai, M. Thitisaksakul, Deciphering rice metabolic flux reprograming under salinity stress via in silico metabolic modeling, Comput. Struct. Biotechnol. J. 18 (2020) 3555–3566, https://doi.org/10.1016/j.csbj.2020.11.023.
A.R. Wellburn, The spectral determination of chlorophylls a and b, as well as total carotenoids, using various solvents with spectrophotometers of different resolution, J. Plant Physiol. 144 (1994) 307–313, https://doi.org/10.1016/S0176-1617(11)81192-2.
Y. Xu, X. Sun, J. Jin, H. Zhou, Protective effect of nitric oxide on light-induced oxidative damage in leaves of tall fescue, J. Plant Physiol. 167 (2010) 512–518, https://doi.org/10.1016/j.jplph.2009.10.010.
S. Yan, Q. Liu, W. Li, J. Yan, A.R. Fernie, Raffinose family oligosaccharides: crucial regulators of plant development and stress responses, Crc. Crit. Rev. Plant Sci. 41 (2022) 286–303, https://doi.org/10.1080/07352689.2022.2111756.
W. Yang, P. Xu, J. Zhang, S. Zhang, Z. Li, K. Yang, X. Chang, Y. Li, OsbZIP60-mediated unfolded protein response regulates grain chalkiness in rice, J. Genet. Genom. 49 (2022) 414–426, https://doi.org/10.1016/j.jgg.2022.02.002.
S. Zhao, Q. Zhang, M. Liu, H. Zhou, C. Ma, P. Wang, Regulation of plant responses to salt stress, Int. J. Mol. Sci. 22 (2021), https://doi.org/10.3390/ijms22094609.